A Foxf1-Wnt-Nr2f1 cascade promotes atrial cardiomyocyte differentiation in zebrafish

Ugo Coppola[1], Jennifer Kenney[1], and Joshua S. Waxman[1,2,3,*]

[1]Molecular Cardiovascular Biology Division and Heart Institute, Cincinnati Children's Hospital Medical Center, Cincinnati, OH 45229, USA.

[2]Developmental Biology Division, Cincinnati Children's Hospital Medical Center, Cincinnati, OH 45229, USA.

[3]Department of Pediatrics, University of Cincinnati, College of Medicine, Cincinnati, OH 45229, USA.

*corresponding author.

Email: joshua.waxman@cchmc.org

Short title: A regulatory network promoting *nr2f1a* expression

Abstract

Nr2f transcription factors (TFs) are conserved regulators of vertebrate atrial cardiomyocyte (AC) differentiation. However, little is known about the mechanisms directing Nr2f expression in ACs. Here, we identified a conserved enhancer 3' to the *nr2f1a* locus, which we call *3'reg1-nr2f1a* (*3'reg1*), that can promote Nr2f1a expression in ACs. Sequence analysis of the enhancer identified putative Lef/Tcf and Foxf TF binding sites. Mutation of the Lef/Tcf sites within the *3'reg1* reporter, knockdown of Tcf7l1a, and manipulation of canonical Wnt signaling support that Tcf7l1a is derepressed via Wnt signaling to activate the transgenic enhancer and promote AC differentiation. Similarly, mutation of the Foxf binding sites in the *3'reg1* reporter, coupled with gain- and loss-of-function analysis supported that Foxf1 promotes expression of the enhancer and AC differentiation. Functionally, we find that Wnt signaling acts downstream of Foxf1 to promote expression of the *3'reg1* reporter within ACs and, importantly, both Foxf1 and Wnt signaling require Nr2f1a to promote a surplus of differentiated ACs. CRISPR-mediated deletion of the endogenous *3'reg1* abrogates the ability of Foxf1 and Wnt signaling to produce surplus ACs in zebrafish embryos. Together, our data support that downstream members of a conserved regulatory network involving Wnt signaling and Foxf1 function on a *nr2f1a* enhancer to promote AC differentiation in the zebrafish heart.

Author Summary

Vertebrate hearts are comprised of atrial chambers, which receive blood, and ventricular chambers which expel blood, whose functions need to be coordinated for proper blood circulation. During development, different genetic programs direct the development of these chambers within the vertebrate heart. Members of a family of genes called *Nr2fs* are conserved regulators of atrial chamber development in vertebrates, with mutations in *Nr2f2* of humans being associated with congenital heart defects affecting the atrium. Here, we examine how the gene *nr2f1a*, which is required for normal atrial chamber development in the model zebrafish, is regulated. Using tools, including transgenic reporter lines and genetic mutants, we identify that factors previously shown to regulate atrial chamber development in mammals have conserved roles regulating a genetic element that promotes *nr2f1a* expression within developing atrial cells. Since there is a lack of understanding regarding regulation of *Nr2f* genes during vertebrate atrial cell development, our work provides insights into the conservation of genetic networks that promote heart development in vertebrates and if perturbed could underlie congenital heart defects.

Introduction

Integrated regulatory networks drive chamber-specific atrial and ventricular cardiomyocyte programs from spatially and temporally defined progenitor populations [1–3]. Key factors within these regulatory networks are nuclear receptor subfamily 2 group F members (Nr2fs; formerly called Coup-tfs), which are critical regulators of vertebrate atrial cardiomyocyte (AC) differentiation during earlier stages of cardiogenesis [4] and subsequently maintain AC identity at later stages [4–6]. Although both Nr2f1 and Nr2f2 paralogs in humans and mice are expressed in ACs [5–7], genetic mapping and functional analysis in cell culture and animal models support that Nr2f2 is the predominant Nr2f that is required for AC differentiation in mammals. In humans, genetic mapping studies have associated mutations in *NR2F2* with structural congenital heart defects (CHDs), including atrioventricular septal defects (AVSDs) [7–9], a malformation predominantly caused by failure of ACs at the venous pole to differentiate and form the atrial septum [10]. Consistent with the necessity of Nr2f2 in mammalian AC differentiation, global *Nr2f2* knockout (KO) mice have small, dysmorphic atrial chambers that lack septa [4]. Furthermore, NR2F2 has a greater requirement promoting atrial differentiation compared to NR2F1 in human embryonic and induced pluripotent stem cell-derived models [11]. In contrast to mammalian Nr2fs, zebrafish *nr2f1a* is the functional homolog of mammalian Nr2f2, as it is required for AC differentiation and the maintenance of AC identity [12,13]. Hence, loss of *nr2f1a* results in zebrafish embryos with small atria reminiscent of the atrial defects of Nr2f2 global KO mice [4,11].

While studies in human stem cell-derived cardiomyocytes and mice cumulatively have demonstrated that Nr2f2 is a critical node within a regulatory network that simultaneously promotes atrial differentiation and represses ventricular differentiation within cardiomyocytes [4,5,11,14], we have limited understanding of the upstream regulation of *Nr2f* genes that lead to the proper differentiation of vertebrate ACs, with a variety of somewhat disparate signals and factors showing they can regulate Nr2f expression. In many *in vivo* and *in vitro* developmental contexts, retinoic acid (RA) signaling, which is required to limit heart size and promote differentiation of the posterior second heart field (SHF) [15–18], is necessary and sufficient to promote *Nr2f1* and *Nr2f2* expression [19–22]. Furthermore, RA signaling is sufficient to induce AC differentiation in many *in vitro* induced pluripotent stem cell protocols [23–25]. However, despite candidate RA response elements and epigenetic changes near the promoter [22], it has not been shown if RA signaling directly regulates *Nr2f*

expression within differentiating ACs [26]. In human embryonic stem cell-derived cardiomyocytes, the TF Isl1, which is required for SHF differentiation, negatively regulates *NR2F1* downstream of RA signaling [27]. Additionally, Tbx20, a conserved regulator of cardiomyocyte proliferation [28], is able to promote *Nr2f2* in the ACs of mice through an evolutionarily conserved enhancer [28]. However, as *Isl1* and *Tbx20* are expressed more broadly, and not specifically expressed in differentiating AC progenitors at the venous pole or differentiated ACs, how these TFs coordinate with other signals to promote Nr2f2 expression in ACs is not clear. Similarly, Hedgehog (Hh) signaling has been shown to be able to promote mouse *Nr2f2* via Gli TFs binding to its promoter *in vitro* [29], although this has not been shown in the heart development. Taken together, it is interesting that many of these factors that regulate Nr2fs, in particular RA and Hh signaling, participate in a regulatory network that controls the timing of SHF progenitor differentiation at the venous pole [30,31]. Elegant work from murine and stem cell models has demonstrated that Hh signaling is an upstream factor in a regulatory network involving RA and Wnt signaling, Foxf1/2 and Tbx5 TFs that controls the proper timing of SHF progenitor differentiation at the venous pole of the heart [30,32]. Loss of most of these factors results in AVSDs in murine models and humans [33,34], again consistent with the failure of proper AC differentiation and the impairment of dorsal mesenchymal protrusion development, which contributes to the atrial septum. Despite this understanding of upstream factors in this regulatory network directing AC differentiation at the venous pole in mammals, the mechanisms promoting Nr2f expression in ACs and if there is a connection to the Hh-dependent regulatory network controlling posterior SHF addition are not understood.

Here, we sought to better understand regulatory networks directing Nr2f expression in the differentiation of ACs. Examining regions of open chromatin from Assay for Transposase-Accessible Chromatin (ATAC)-seq analysis of embryonic ACs [35] that were conserved within vertebrates [13], we identified an enhancer 3' to the *nr2f1a* locus, which we named *3'reg1-nr2f1a* (*3'reg1*), that was able to promote expression within ACs of stable transgenic lines. A Lef/Tcf binding site and multiple Foxf binding sites were found within the enhancer. Mutation or deletion of the Left/Tcf site led to ectopic *3'reg1* reporter activation within the heart, while mutation or deletion of the Foxf sites led to decreased *3'reg1* reporter expression within ACs. Complementary gain- and loss-of-function experiments manipulating Wnt signaling and Foxf1 coupled with epistasis analysis support a model

107 whereby Wnt signaling, which functions at the level or downstream of Foxf1, relieves Tcf7l1a-
108 mediated repression of the *3'reg1* enhancer and promote AC differentiation. However, in contrast to
109 the established role of Hh signaling functioning upstream of these factors in venous SHF
110 differentiation in mammals, Hh was found to modestly repress transgenic *3'reg1* reporter expression
111 and did not affect AC differentiation. Consistent with Nr2f1a functioning downstream of Wnt signaling
112 and Foxf1, neither is sufficient to promote a surplus of ACs in zebrafish *nr2f1a* mutants. Furthermore,
113 CRISPR-mediated deletion of the endogenous *3'reg1* enhancer showed that this abrogated the ability
114 of Wnt signaling and Foxf1 to enhance the number of differentiated ACs. Cumulatively, our results
115 support that downstream components of a regulatory network involving Wnt signaling and Foxf1,
116 which control differentiation of the SHF in mammals, promote AC differentiation via directing zebrafish
117 *nr2f1a* expression through a conserved 3' enhancer.

118 **Results**

119 **A *nr2f1a* enhancer drives expression in ACs**

120 To decipher regulatory networks that control *Nr2f* gene expression with respect to its role in
121 heart development, we first examined ~1.5 kb upstream of the transcription start site (TSSs) of *nr2f1a*
122 as well as the 5'-untranslated region (5'-UTR) for the ability to promote expression in ACs (**S1A Fig.**
123 **and S1 Table**). Only 1.5 kb upstream were chosen as to not include an adjacent lincRNA, which could
124 complicate analysis. The 5'-UTR was included because we previously identified a conserved RA
125 response element in the *nr2f1a* 5'-UTR [13]. Five different constructs encompassing the 1.5 kb of the
126 *nr2f1a* promoter and different lengths of 5'-UTR were examined with reporter vectors driving GFP
127 (**S1A-F Fig.**). In stable transgenic lines, all the cloned regions showed similar broad expression
128 throughout the embryos, including in the nervous system, somites, and the heart (**S1B-F Fig.**).
129 Additionally, the promoter constructs were not responsive to manipulation of RA signaling (data not
130 shown). Thus, regulatory elements contained within the proximal promoter do not appear to drive
131 *nr2f1a* expression specifically in ACs, consistent with the broader transcriptional regulation generally
132 found with proximal promoters [36], and more distal *cis*-regulatory elements (CREs) likely promote
133 AC-specific *nr2f1a* expression in zebrafish.

134 Given the conservation of their expression within ACs, we next postulated that *Nr2f* genes
135 might have conserved CREs that promote their AC expression. To identify conserved CREs that
136 promote expression specifically in the ACs, we examined regions of open chromatin found in our
137 recently reported ATAC-seq on isolated ACs from 48 hours post-fertilization (hpf) embryos [35] for
138 conservation using genomic alignments of all vertebrate *Nr2f1* loci with VISTA plots (**Fig. 1A-C and**
139 **S2A,B,D,F,H Fig.**). Although there is a conserved gene desert 5' to vertebrate *Nr2f* genes, we did not
140 find conservation of sequences within regions of open chromatin in the ~700kb 5' distal the zebrafish
141 *nr2f1a*. The regions of open chromatin with conserved sequence in vertebrate genomes were
142 primarily within ~20kb 5' and 3' of the *nr2f1a* locus, with the conservation in 3' regions of open
143 chromatin extending to the syntenic gene *fam172a* [37] (**S2A Fig.**). We identified 7 conserved open
144 regions flanking *nr2f1a* (**Fig. 1A-C**, **S2A,B,D,F,H Fig., and S3A-D Fig.**), which were subsequently
145 analyzed via cloning into a GFP reporter vector [38]. Two of the putative enhancers did not drive
146 significant GFP expression in transient transgenic embryos and were not studied further. The rest of

147 the putative enhancers were named according to their 5' and 3' positions relative to *nr2f1a* (**Fig. 1A**
148 **and S2A Fig.**). Those that did drive tissue-specific expression in transient transgenics were raised to
149 confirm their expression in stable transgenic lines. Two of the transgenic enhancer reporters showed
150 expression within subdomains that are reminiscent of the endogenous extra-cardiac *nr2f1a*
151 expression [39]. *5'reg1-nr2f1a* was expressed in the anterior hindbrain and branchial arches (**S2C**
152 **Fig.**). *3'reg4-nr2f1a* was expressed in the medial eye, nasal pits, and anterior branchial arch (**S2I**
153 **Fig.**). Two putative enhancers, *3'reg2-nr2f1a* and *3'reg3-nr2f1a,* were expressed within the heart by
154 48 hpf, but did not show atrial-specific expression (**S2E,G Fig.**). However, the *3'reg1-nr2f1a* enhancer
155 (henceforth referred to as *3'reg1*) showed expression specifically within ACs by 24 hpf, which was
156 maintained through 72 hpf (**Fig. 1D-H**). Moreover, the strongest expression of the *3'reg1* reporter was
157 at the venous pole of the atrium and it tapered toward the atrioventricular canal/outflow pole of the
158 atrium (**Fig. 1E-H**). Although *nr2f1a* expression is first detectable by early somitogenesis stages in
159 the ALPM [13], with the present analysis we did not identify CREs that drove expression during earlier
160 stages in the ALPM. Thus, we identified a conserved putative *nr2f1a* enhancer that is able to promote
161 expression within zebrafish ACs by the early heart tube stage.
162
163 **Wnt signaling promotes Nr2f1a expression in ACs**
164 To determine signals that could regulate *3'reg1*, we performed TF binding site (TFBS) analysis
165 using the CIS-BP [40,41], TomTom [42,43], and JASPAR [44] databases. Among the different
166 putative TFBSs identified within *3'reg1* were a nuclear hormone receptor (NHR) binding site, a Lef/Tcf
167 binding site, and multiple Foxf binding sites (**Fig. 1C and S4A Fig.**), reflecting signals, including RA
168 and Wnt signaling, that are involved in promoting the proper timing of AC differentiation from the
169 posterior SHF progenitors in mice [15,16,32,45]. Furthermore, there was enriched conservation of
170 nucleotides in the regions of the enhancers harboring the potential binding sites, although there was
171 less conservation over the putative Lef/Tcf binding site (**Fig. 1C**). We next systematically interrogated
172 the requirement of each of these sites in promoting *3'reg1:GFP* expression in ACs. Since RA signaling
173 potentially regulates *Nr2f* expression during atrial differentiation [13,25,46], we initially examined the
174 requirement of the NHR site (**S4A-C Fig.**). However, deletion of the NHR site did not alter expression
175 of the reporter compared to the unaltered *3'reg1:GFP* reporter in transient transgenic embryos nor

176 did modulation of RA signaling via treatment with RA and the RA signaling inhibitor DEAB affect
177 expression in stable transgenic *3'reg1:GFP* lines (data not shown**).** Therefore, RA signaling does not
178 appear to regulate *nr2f1a* expression through this enhancer.

179 Lef/Tcf TFs are mediators of canonical Wnt signaling [47,48], with numerous *in vivo* and *in*
180 *vitro* studies having shown it controls differentiation of ACs [49,50]. Furthermore, we have shown that
181 increased Wnt signaling during later somitogenesis immediately prior to the formation of the heart
182 tube is necessary and sufficient to specifically produce an increase in ACs in zebrafish embryos [51].
183 Additionally, studies have demonstrated that Wnt signaling is expressed in a gradient extending from
184 the venous pole of the zebrafish heart [51–53], which is reminiscent of the *3'reg1:GFP* reporter. We
185 found that either deletion or targeted mutation of the Lef/Tcf site both resulted in an expansion of the
186 reporter throughout the heart by 48 hpf relative to the *3'reg1:GFP* in transient transgenic embryos
187 (**Fig. 2A-F**). As this result suggests the site may be used to restrict enhancer expression, we reasoned
188 that Tcf7l1a (formerly called Tcf3a), a transcriptional repressor whose repression is relieved by Wnt
189 signaling [54] that we have previously implicated in early cardiomyocyte development [53], may be
190 limiting the expression of the reporter within the heart at these stages of cardiogenesis. To determine
191 if Tcf71a limits expression of the reporter, *3'reg1:GFP* embryos were injected with an established
192 morpholino (MO) that identically phenocopies the zebrafish *tcf7l1a* mutants [55]. We found that
193 Tcf7l1a depletion produced pan-cardiac expression of the *3'reg1:GFP* reporter (**Fig. 2G-I**), supporting
194 that Tcf7l1a is required to limit *3'reg1* reporter expression within the heart.

195 As the activation of the transgenic *3'reg1:GFP* reporter via Tcf7l1a depletion would predict
196 Wnt signaling should also regulate the *3'reg1:GFP* reporter expression within the heart, we
197 manipulated Wnt signaling in *3'reg1:GFP* embryos at the 20 somite (s) stage with treatments of BIO
198 and XAV939 (XAV), which respectively activate and inhibit Wnt signaling [56]. The 20s stage was
199 chosen because we previously found that modulation of Wnt signaling could specifically affect AC
200 number slightly prior to this stage at ~16s [51,53]. Although the effect of Wnt signaling on AC
201 differentiation was not examined previously at the 20s stage, this stage was also just prior to when
202 we can detect transgenic *3'reg1:GFP* reporter expression. We found that by 48 hpf the hearts of the
203 embryos treated with BIO showed pan-cardiac GFP expression (**Fig. 3A,B,D**), similar to perturbation
204 of the Lef/Tcf sites in the *3'reg1:GFP* reporter (**Fig. 2C-E**) and Tcf7l1a depletion (**Fig. 2G,H**), while

205 XAV abrogated GFP expression within the atria (**Fig. 3A,C,D**). Since our data supported that Wnt
206 signaling activates the *3'reg1:GFP* reporter, likely via derepression of Tcf7l1a [53], we tested if Wnt
207 signaling at these stages impacts Nr2f1a expression within the heart. As a proxy for affecting Nr2f1a
208 expression, we quantified the number of Nr2f1a$^+$ cardiomyocyte nuclei within the hearts of 48 hpf
209 embryos treated with BIO and XAV beginning at the 20s stage (**Fig. 3E-H**). Although we did not
210 observe obvious ectopic Nr2f1a expression within ventricular cardiomyocytes (VCs) as with the
211 *3'reg1:GFP* reporter, BIO treatment at the 20s stage produced a surplus of Nr2f1a$^+$/Ahmc$^+$
212 cardiomyocytes (ACs) by 48 hpf. Conversely, XAV treatment caused a decrease in Nr2f1a$^+$/Amhc$^+$
213 cardiomyocytes (ACs) within the atrium, with the Amhc$^+$ ACs qualitatively having a reduction in Nr2f1a
214 expression within their nuclei. Based on the effects of Wnt signaling on Nr2f1a in ACs and our
215 previous observations that manipulation of Wnt signaling at similar somitogenesis stages specifically
216 affected AC production [51], we tested the impact of Wnt manipulation on ACs using the
217 *myl7:DsRed2-NLS* transgene [57]. In agreement with the assessment of Nr2f1a$^+$ cardiomyocytes,
218 BIO and XAV treatment at the 20s stage respectively produced a surplus and decrease in the number
219 of ACs (*myl7:*DsRed2-NLS$^+$/Amhc$^+$ cardiomyocytes) by 48 hpf (**Fig. 3I-L**). However, we did not detect
220 changes in the number of VCs (**S5A Fig.**), similar to what we have reported previously [51,53]. Thus,
221 Wnt signaling is necessary and sufficient at the 20s stage to activate the transgenic *3'reg1:GFP*
222 reporter and promote a surplus of differentiated ACs, likely through derepression of Tcf7l1a.
223

224 **Foxf1 promotes Nr2f1a expression in ACs**

225 In mice, Foxf1 and Foxf2 TFs control the proper differentiation of posterior SHF progenitors
226 downstream of Hh signaling [30,58]. Thus, we were intrigued by the conserved Foxf sites within the
227 *3'reg1* enhancer (**Fig. 1C**). We found that in transient transgenic embryos deletion or mutation of each
228 of the 3 Foxf binding sites diminished the percentage of embryos with GFP in their atria relative to
229 injection of the wild-type (WT) *3'reg1* reporter (**Fig. 4A-C**), suggesting the putative Foxf sites may be
230 required to promote *3'reg1:GFP* expression. To further test this hypothesis, murine *Foxf1* mRNA was
231 injected into *3'reg1:GFP* transgenic embryos. We found Foxf1 was sufficient to expand and promote
232 *3'reg1:GFP* expression into VCs by 48 hpf (**Fig. 4D,E,G**). Conversely, injecting a dominant-negative
233 murine *Foxf1* (*dnFoxf1*) mRNA into the *3'reg1:GFP* transgenic embryos was able to inhibit reporter

234 expression within the heart (**Fig. 4D,F,G**). Although zebrafish mutants for *foxf1* have been described
235 [59], if they have cardiac defects was not reported. Nevertheless, we sought to determine if *foxf1* is
236 required for *3'reg1:GFP* reporter expression and we targeted zebrafish *foxf1* using the CRISPR-
237 Cas12a system [60–62] with guides we found were highly efficient in creating deletions (**S6A,B Fig.**).
238 Although we did not observe overt cardiac defects, injection of the *foxf1* CRISPRs was sufficient to
239 reduce expression of the *3'reg1:GFP* reporter in transgenic embryos (**S6C-E Fig.**). Given the effects
240 on the *3'reg1:GFP* reporter, we asked if Foxf1 was sufficient to promote Nr2f1a$^+$ ACs and increase
241 the number of differentiated ACs. We found that embryos injected with *Foxf1* or *dnFoxf1* mRNA
242 respectively showed increases and decreases in both Nr2f1a$^+$/Amhc$^+$ and *myl7:DsRed2-NLS*$^+$/Amhc$^+$
243 cardiomyocytes within their hearts at 48 hpf (**Fig. 4H-O**), without affecting the number of VCs (**S5B**
244 **Fig.**). As with Wnt inhibition, embryos injected with the *dnFoxf1* mRNA qualitatively had reduced
245 expression of Nr2f1a within the atrium at 48 hpf (**Fig. 4J**). Thus, our data suggest that Foxf1 can
246 activate the transgenic *3'reg1:GFP* reporter and promote an increase in differentiated Nr2f1a-
247 expressing ACs.
248
249 **Hh signaling represses *3'reg1* reporter expression**
250 In mice, Hh signaling has been established as a key regulator of posterior SHF differentiation
251 upstream of factors, including Foxf1 and Foxf2, and Wnt signaling [29–31], and has previously been
252 implicated in regulating Nr2f2 expression in P19 cells [63]. Thus, we asked if Hh signaling could affect
253 the *3'reg1:GFP* reporter within the atria. Transgenic *3'reg1:GFP* embryos were treated with the Hh
254 signaling inhibitor Cyclopamine (CYA) [64] and the Hh signaling activator SAG [65] beginning at the
255 20s stage, which is after previous reports demonstrated that Hh signaling affects the production of
256 cardiac progenitors [55]. However, in contrast to the effects of Wnt and Foxf1 manipulation, embryos
257 treated with CYA at the 20s stage unexpectedly showed a modest expansion of the *3'reg1:GFP*
258 reporter within the atrium, while SAG-treated *3'reg1:GFP* embryos showed a reduction of *3'reg1*:GFP-
259 expression (**S7A-D Fig.**). To confirm that Hh signaling represses *3'reg1:GFP* reporter expression, we
260 examined the *3'reg1:GFP* reporter in *smoothened* (*smo)* mutants. Consistent with CYA treatments,
261 we found a modest expansion of the *3'reg1:GFP* reporter within the atria of *smo* mutants (**S7E-G**
262 **Fig.**). However, despite the effects on the *3'reg1:GFP* reporter within the atrium, modulation of Hh

263 signaling did not affect the number of Nr2f1a$^+$ ACs (**S7H-K Fig.**). As Hh signaling may be upstream
264 of Wnt signaling in posterior SHF differentiation in mammals [31,66], we also concurrently
265 manipulated Wnt and Hh signaling at the 20s stage with the aforementioned drugs. We found that
266 simultaneously inhibiting or activating Wnt and Hh signaling on decreased and increased expression
267 of the *3'reg1:GFP* reporter within the heart, similar to inhibiting or activation of Wnt signaling alone
268 (**S7L-O Fig.**). Therefore, our data suggest that in contrast to mammalian venous pole differentiation
269 Hh signaling is likely not affecting AC differentiation at these stages of cardiogenesis nor is it
270 promoting Nr2f expression in ACs upstream of Wnt or Foxf1 in zebrafish embryos.
271
272 **Wnt signaling functions downstream of Foxf1**
273 To decipher the functional relationship between Wnt signaling/Tcf7l1a and Foxf1 on activation
274 of the *3'reg1:GFP* reporter within the atrium, we simultaneously manipulated these signals within the
275 transgenic embryos. While *3'reg1:GFP* embryos injected with *Foxf1* mRNA had pan-cardiac
276 expression, the majority of *Foxf1* mRNA-injected *3'reg1:GFP* embryos treated with XAV at the 20s
277 stage lose *3'reg1:GFP* reporter expression within the atrium by 48 hpf, similar to XAV treatments
278 alone (**Fig. 5A-E**). We next simultaneously injected *Foxf1* and zebrafish *tcf7l1a* mRNAs into the
279 *3'reg1:GFP* embryos. Consistent with the Tcf7l1a functioning as a repressor, *tcf7l1a* overexpression
280 abrogated *3'reg1:GFP* reporter expression within the atrium (**Fig. 5F,H,J**). When both TFs were co-
281 overexpressed in *3'reg1:GFP* embryos, we did not observe pan-cardiac expression of the *3'reg1:GFP*
282 reporter within the atrium at 48 hpf (**Fig. 5F-J**). Next, we co-injected the *tcf7l1a* MO and *dnFoxf1*
283 mRNA into the *3'reg1:GFP* embryos. In this scenario, we found that the *dnFoxf1* was not sufficient to
284 block the pan-cardiac expression induced by Tcf7l1a depletion (**Fig. 5K-O**). Since these data
285 suggested that Wnt signaling may function downstream of Foxf1, we asked if Foxf1 was sufficient to
286 promote an increase in Wnt signaling within embryos. RT-qPCR on 24 hpf embryos injected with
287 *Foxf1* mRNA promoted a modest but significant increase in the expression of *axin1*, a Wnt responsive
288 gene that negatively regulates canonical Wnt signaling [67] , and a decrease in the expression of the
289 Wnt signaling inhibitor *dkk1a* [67] (**S8A,B Fig.**). Cumulatively, these data suggest that Wnt signaling
290 functions downstream, or parallel, to Foxf1 in the activation of the *3'reg1:GFP* reporter.
291

292 **Wnt signaling and Foxf1 require Nr2f1a to promote surplus ACs**

293 Nr2f1a is required for AC differentiation within the early zebrafish heart [12]. As our results
294 support that enhanced Wnt signaling and Foxf1 are sufficient to promote more differentiated ACs, we
295 asked if this ability was dependent on Nr2f1a. Embryos resulting from crosses of *nr2f1a*$^{+/-}$ fish that
296 carry the *myl7:DsRed2-NLS* transgene were treated with BIO at the 20s stage. We found that BIO
297 treatment was not sufficient to produce an increase of ACs in 48 hpf *nr2f1a* mutants, while it was
298 sufficient to produce an increase in the number of ACs in their WT siblings (**Fig. 6A-E**). Similarly,
299 injection of *Foxf1* mRNA into embryos resulting from crosses of *nr2f1a*$^{+/-}$ fish that carry the
300 *myl7:DsRed2-NLS* transgene showed that *Foxf1* mRNA was no longer sufficient to produce a surplus
301 of ACs in *nr2f1a* mutants, unlike their control sibling embryos (**Fig. 6F-J**). Thus, our data support that
302 Nr2f1a is required for Wnt signaling and Foxf1 to be sufficient to promote a surplus of ACs.

303

304 **Wnt signaling and Foxf1 require *3'reg1* to promote ACs**

305 Since the *3'reg1:GFP* reporter is expressed in ACs, we wanted to determine if the endogenous
306 *3'reg1* enhancer is required *in vivo* to promote or maintain Nr2f1a expression in ACs. Therefore, we
307 deleted the endogenous *3'reg1* enhancer in zebrafish using a CRISPR-Cas12a system [68] (**Fig. 7A**
308 **and S9A,B Fig.**). We found that embryos with homozygous deletion of the endogenous *3'reg1*
309 enhancer overtly did not show defects (**S9C,D Fig.**). Furthermore, there was no difference in the
310 number of ACs (Nr2f1a^{+}/Amhc^{+} cardiomyocytes) in the hearts of *3'reg1* deletion mutants compared
311 to their WT sibling embryos at 48 hpf (**Fig. 7B,C,F,G,H,K**), suggesting that *in vivo* deletion of the
312 *3'reg1* enhancer alone is not sufficient to abrogate proper N2f1a expression within the atrium.
313 Consequently, we then asked if Wnt signaling and Foxf1 require the endogenous *3'reg1* enhancer to
314 be able to produce a surplus of Nr2f1a^{+} ACs. We found that both BIO treatment and Foxf1 mRNA
315 injection were unable to produce a surplus of Nr2f1a^{+}/Amhc^{+} cardiomyocytes within the hearts of
316 homozygous *3'reg1* deletion mutants (**Fig. 7B-K**). Overall, these data suggest that the endogenous
317 *3'reg1* is required to mediate the sensitivity of Nr2f1a and AC differentiation to Wnt signaling and
318 Foxf1 in the zebrafish atrium.

319 **Discussion**

320 In the present study, our data show that in zebrafish embryos Wnt signaling and Foxf1 function
321 upstream of Nr2f1a in promoting AC differentiation via regulating a conserved *Nr2f1* enhancer, which
322 is located ~2.5kb 3' to zebrafish *nr2f1a* (**Fig. 8**). Previous work has placed both these signals
323 downstream of Hh signaling in a regulatory network that controls the differentiation of ACs from the
324 posterior SHF in mice [31,32,66]. Thus, our data support that there are conserved roles for these
325 downstream factors in promoting the proper number of differentiated ACs in the hearts of vertebrates.
326 Numerous studies have investigated the different roles of canonical Wnt signaling in cardiac
327 development in mice, zebrafish, and stem cells [32,33,47,53,69]. Furthermore, our previous study
328 examining the temporal requirements of Wnt signaling in zebrafish showed that it is necessary and
329 sufficient to specifically promote surplus ACs during later somitogenesis immediately prior to the
330 formation of the heart tube [51,53], a time point when posterior SHF progenitors are adding to the
331 zebrafish heart [70]. Additional work in zebrafish has shown that Wnt signaling at the lateral borders
332 of the heart field and at the venous pole is required for the differentiation of pacemaker
333 cardiomyocytes [71]. Our present study corroborates the role for Wnt signaling in promoting the proper
334 number of ACs as the heart tube is forming during late somitogenesis, which we propose is through
335 affecting the differentiation of ACs from the zebrafish posterior SHF. Furthermore, our work supports
336 that the ability of Wnt signaling to promote ACs necessitates Nr2f1a, whose expression is regulated
337 via the derepression of Tcf7l1a.

338 Despite the established roles of Foxf1/2 TFs in regulating differentiation of the posterior SHF
339 in mice [58,72,73], if Foxf TFs play similar roles in zebrafish heart development has not been
340 investigated. Previous work examining Foxf factors in zebrafish demonstrated redundant
341 requirements for Foxf1/2 TFs in craniofacial development [59,74]. Similar to the roles of Foxf1/2 in
342 mice [30,58,72], our data suggest that the Foxf TFs are necessary and sufficient to promote the
343 formation of ACs in zebrafish embryos. Although our data did not yet specifically address the temporal
344 or spatial requirements of Foxf factors, the necessity of Nr2f1a in promoting the proper number of
345 differentiated ACs would also support a model that affects the differentiation of zebrafish posterior
346 SHF progenitors. Thus, as with Wnt signaling, our data support a conserved requirement for Foxf TFs
347 upstream of Nr2f1a in controlling the differentiation of ACs at the venous pole in vertebrates. However,

348 although we found that depletion of *foxf1* affected the expression of the *3'reg1:GFP* reporter, zebrafish
349 *foxf1* crispants did not overtly have cardiac defects. Similarly, Wnt signaling and Foxf1 could induce
350 ectopic *3'reg1:GFP* reporter in VCs, but neither were able to induce ectopic Nr2f1a in VCs. Hence,
351 the reporter may be more sensitive to manipulation of Wnt signaling and Foxf factors than
352 endogenous Nr2f1a due to a lack of input from additional CREs. Nevertheless, we postulate that
353 multiple *foxf* factors in zebrafish likely function redundantly to promote AC differentiation of zebrafish,
354 as with Foxf1/2 in mice [58,72], which will be investigated more in the future.

355 Integrating how Wnt signaling and Foxf TFs function upstream of Nr2f1a, our analysis
356 supports that Wnt signaling, via derepression of Tcf7l1a, functions downstream, or at the level, of
357 Foxf1. This functional relationship is reminiscent of other developmental contexts, such as
358 osteogenesis [75,76], where Foxf factors have been found to regulate the canonical Wnt signaling
359 pathway [77]. Despite their functional relationship in promoting the differentiation of zebrafish ACs,
360 we have not determined the specific mechanism by which Foxf factors regulate Wnt signaling in this
361 context. Given the adjacent Foxf sites and Lef/Tcf site within the *3'reg1* CRE, one might predict that
362 Foxf factors, which can act as pioneer factors [78,79], facilitate the derepression of Tcf7l1a via making
363 the CRE accessible to Wnt signaling. However, our data would argue against this model, as we find
364 Tcf7l1a does not appear to require Foxf for the derepression. Another possibility is that Foxf reinforces
365 the activation of the CRE via simultaneously acting on the *3'reg1* enhancer and independently
366 promoting Wnt signaling via derepression of Tcf7l1a. Additionally, while Foxf1 can function as a
367 transcriptional activator [80], it is predominantly known as a transcriptional suppressor [81,82]. The
368 dependence of the *3'reg1:GFP* reporter on the putative Foxf sites would minimally suggest that in this
369 context these sites are being utilized by a transcriptional activator, which correlates with the evidence
370 that Foxf1 is able to promote *3'reg1:GFP* reporter expression and atrial differentiation. Nevertheless,
371 we acknowledge that in the absence of evidence for direct binding to the endogenous *3'reg1*
372 enhancer, other scenarios are plausible, including that Foxf1 represses a Wnt inhibitor. However, in
373 mice, in addition to repression of factors that limit differentiation of the posterior SHF, Foxf1/2 are also
374 required for the activation of chamber-specific differentiation programs [30] which could also suggest
375 that it has dual functions as a repressor and activator in this context.

376 In mammals, Hh signaling sits atop a regulatory network that controls the proper timing of
377 differentiation from posterior SHF progenitors through Tbx5 and Foxf TFs, and Wnt and RA signaling
378 [30,32,69]. Although our data support that downstream factors in this regulatory network, Wnt
379 signaling and Foxf TFs, are conserved in regulating posterior SHF addition in zebrafish, our data and
380 previous studies do not support the conservation of the upstream factors [30,31]. Previous work
381 established that in zebrafish Hh signaling is required during early patterning stages to promote the
382 proper number of differentiated ACs and VCs [55], while a requirement at later stages of
383 somitogenesis and posterior SHF addition equivalent to those examined in this study was not found.
384 Consistent with the previous observations of the temporal requirements of Hh signaling [55,83], we
385 did not find it was required upstream of Wnt signaling or Foxf. Instead, we found that there was a
386 minimal effect of Hh signaling repressing the *3'reg1:GFP* reporter, which was the opposite of what
387 would be expected from the mammalian data. Furthermore, we did not find evidence that Hh regulates
388 Nr2f1a or affects the number of differentiated ACs in zebrafish during late somitogenesis and early
389 heart tube formation. Previous work has also established that Tbx5, which functions downstream of
390 Hh and RA signaling in mice in posterior SHF differentiation [30–32], is not required for zebrafish atrial
391 differentiation [84–86]. It is interesting to consider the lack of conservation of these upstream factors
392 in the regulation of the vertebrate posterior SHF. The posterior SHF-derived cells that contribute to
393 the single atrium and venous pole in zebrafish are significantly less than that found in mice [70,83].
394 By virtue of its lack of requirement, our work would support the proposed hypothesis whereby
395 heterochrony of a Hh-dependent regulatory network may have contributed to the enlargement of the
396 posterior SHF and the concurrent the evolution of the pulmonary system in air-breathing vertebrates
397 [69,83].

398 Specifically evaluating the *3'reg1* enhancer, our data support that it is highly conserved among
399 vertebrates, but is absent in agnathans (hagfish and lamprey) and birds. A lack of this CRE in
400 agnathans could suggest that it evolved beginning in cartilaginous fishes. Although not explored here,
401 *Nr2f2* genes, which diverged from *Nr2f1* early in the vertebrate lineage [37], also have a conserved
402 putative enhancer located in a similar region (**S10 Fig.**), suggesting these enhancers may have had
403 a similar origin at least in agnathans prior to the divergence of these paralogs. Although the *Nr2f1*
404 *3'reg1* is lost in birds, the conservation of the putative *Nr2f2-3'reg1* within birds could reflect the

405 greater reliance of *Nr2f2* within their hearts similar to its role in mammals. The general conservation
406 of the *3'reg1* in vertebrates is interesting in light that it has been suggested that CREs regulating
407 cardiac expression are actually poorly conserved in vertebrates [87]. Additionally, deletion of the
408 *3'reg1* did not cause overt loss of or failure to maintain Nr2f1a and ACs deficits. Thus, other CREs
409 are likely involved in or compensate for the loss of the *3'reg1*, which is not uncommon [88], and may
410 also be a reason its loss could be tolerated in agnathans and birds. We focused on the *3'reg1* because
411 of the functional importance of *nr2f1a* in zebrafish atrial differentiation. Our data support that Wnt
412 signaling and Foxf factors require the endogenous *3'reg1* enhancer to be able to augment the number
413 of ACs, even if the element itself is not required to promote or maintain normal Nr2f1a expression
414 within the heart. Furthermore, although this was the only conserved *Nr2f1* CRE thus far that we
415 identified promotes AC-specific expression, we did find nearby CREs that promoted expression more
416 broadly in cardiomyocytes. We have not yet examined the coordination of these CREs and if
417 expression driven with the region 3' to *nr2f1a* encompassing all the CREs better reflects endogenous
418 *nr2f1a* within ACs. Additionally, as the transgenic *3'reg1* reporter expression initiates at early heart
419 tube stages, which is later than endogenous *nr2f1a* expression occurs in the anterior lateral plate
420 mesoderm during early somitogenesis, and demonstrates a graded pattern, this would suggest that
421 this enhancer is required to promote or maintain *nr2f1a* expression within more venous ACs at later
422 stages.

423 In summary, our data have provided insights into a Foxf-Wnt-Nr2f regulatory network that
424 determines the number of differentiated ACs within the zebrafish heart. Our study has implications for
425 our understanding of the development and evolution of gene regulatory networks controlling posterior
426 SHF and AC differentiation in vertebrates and given the conserved requirements of Nr2f factors could
427 be used to inform us of mechanisms underlying congenital heart defects that affect the atria in
428 mammals. Future studies will be aimed at deciphering the specific transcriptional mechanisms that
429 control the logic of this regulatory network and expanding our analysis to additional CREs directing
430 *Nr2f1* and *Nr2f2* expression in ACs.

Funding

Work in the manuscript was supported by National Institutes of Health (NIH) grants R01 HL168790 and R01 HL137766 to J.S.W., by American Heart Association (AHA) postdoctoral fellowship 831018 to U.C., and by AHA Summer Undergraduate Research Fellowship (SURF) grant 18UFEL33930019 to J.K.. The funders had no role in study design, data collection and analysis, decision to publish, or preparation of the manuscript.

Acknowledgements

We thank Kendall Martin for technical assistance, training, and reading of the manuscript.

441 **Materials and Methods**

442 **Ethics statement**

443 All zebrafish husbandry and experiments were performed following protocols approved by the
444 Institutional Animal Care and Use Committee (IACUC) of Cincinnati Children's Hospital Medical
445 Center (Protocol IACUC2023-1048).

446

447 **Zebrafish husbandry and lines used**

448 Adult zebrafish were raised and maintained under standard laboratory conditions [89]. WT fish
449 used were mixed AB-TL background. Transgenic and mutant lines used were: *Tg(-*
450 *1.5_nr2f1a:GFP)*^{ci1020}, *Tg(-1.4_nr2f1a:GFP)*^{ci1021}, *Tg(-0.7s_nr2f1a:GFP)*^{ci1022}, *Tg(-*
451 *0.7m_nr2f1a:GFP)*^{ci1023}, *Tg(-0.7l_nr2f1a:GFP)*^{ci1024}, *Tg(5'reg1-nr2f1a:GFP)*^{ci1025}, *Tg(3'reg1-*
452 *nr2f1a:GFP)*^{ci1026}, *Tg(3'reg2-nr2f1a:GFP)*^{ci1027}, *Tg(3'reg3-nr2f1a:GFP)*^{ci1028}, *Tg(3'reg4-*
453 *nr2f1a:GFP)*^{ci1029}, *Tg(−5.1myl7:DsRed2-NLS)*^{f2} [57], *Tg(-5.1myl7:EGFP)*^{twu26} [90], *smo*^{s294} [91],
454 *nr2f1a*^{ci1009} [35].

455

456 **Analysis of *Nr2f* loci and TFBS analysis**

457 ATAC-seq data used in this study on flow-sorted zebrafish ACs at 48 hpf and alignments
458 shown were reported previously (GEO, Accession # GSE 194054) [35]. Regions of open chromatin
459 700 kb upstream (a gene desert) and 18 kb downstream of the *nr2f1a* zebrafish locus were initially
460 examined within the UCSC browser (https://genome.ucsc.edu). Open chromatin in these regions of
461 the zebrafish genome adjacent to the *nr2f1a* locus that appeared to have conservation based on
462 alignments with genomes available in the UCSC genome browser were selected for additional
463 analysis of conservation through alignments using mVista
464 (http://genome.lbl.gov/vista/mvista/submit.shtml) and subsequent reciprocal nBLASTs on Ensembl
465 (Ensembl.org). Specific sequences from species corresponding to the conserved regions of open
466 chromatin flanking *Nr2f1* loci in other species were retrieved from Ensembl: Australian ghostshark
467 (*Callorhinchus_milii*-6.1.3), Tropical clawed frog (UCB_*Xtro*_10.0), Green anole (*AnoCar*2.0v2),
468 Chicken (bGalGal1.mat.broiler.GRCg7b), House mouse (GRCm39), and Human (GRCh38.p14). The
469 conserved regions in the different species, corresponding to the open chromatin in the zebrafish ACs,

470 were manually aligned using Clustal Omega [92]. Sequences with a high degree of conservation from
471 the alignment were analyzed for the presence of conserved TFBS using CIS-BP [40,41] , TomTom
472 [42,43], and JASPAR databases [44].
473
474 **Cloning of Plasmids**
475 The *nr2f1a* promoter and enhancer reporters were generated using established Gateway
476 cloning methods [93]. The designated regions of the *nr2f1a* promoter were cloned into *pDONR P4-*
477 *P1r* to generate 5'-entry clones. Subsequently, each of the *p5E-nr2f1a* promoter clones were
478 combined with *pME-EGFP* middle-entry and *p3E-polyA* 3'-entry clones into the previously reported
479 *pDestTol2p2a-cry:DsRed* destination vector [93] to generate the *nr2f1a* promoter reporter constructs.
480 The putative enhancer regions were cloned into the *pE1b-GFP-Tol2-Gateway* vector (Addgene,
481 plasmid # 37846) [38]. A QuickChange Site-Directed Mutagenesis Kit (Agilent, Cat # 200524) was
482 employed to generate the designated deletions and mutations of the putative binding sites within the
483 *3'reg1-nr2f1a:GFP* reporter vector. Primers used for cloning are listed in **S2 Table**.
484 The murine *Foxf1* construct (gift of V. Kalinichenko) was reported previously [72]. The
485 construct contains N-terminal Flag and C-terminal His tags. This construct was subcloned into
486 *pCS2p+DEST1*, a version of *pCS2-Dest1* [94] with a Pst1 site added, using Gateway cloning. The
487 *dnFoxf1* expression construct was generated via fusing the Engrailed transcriptional repressor
488 domain with a 21 bp linker to the 5'-end of the murine *Foxf1* construct using PCR and placed into the
489 *pCS2p+DEST1* vector.
490
491 **Morpholino (MO), mRNA, and plasmid injections**
492 The *tcf7l1a* (aka *tcf3a*) MO was reported previously [95]. 1 ng of *tcf7l1a* MO was injected.
493 mRNAs for *Foxf1*, *dnFoxf1*, and zebrafish *tcf7l1a [54]* were generated from linearized plasmid using
494 a Sp6 Message Machine kit (Thermo-Fisher, Cat # AM1340). 50 pg of mRNA for *Foxf1* and *dnFoxf1*
495 were injected. 5 pg of zebrafish *tcf7l1a* was injected. All injections were performed at the one-cell
496 stage.
497
498 **Generation of transgenic lines**

499 *Tol2* mRNA was generated from linearized plasmid using a Sp6 Message Machine kit
500 (Thermo-Fisher, Cat # AM1340) [93]. For transient transgenesis and the generation of stable
501 transgenic lines, 25 pg of plasmid DNA was co-injected with 25 pg of *Tol2* mRNA. For stable
502 transgenic lines, fish were raised to adulthood and founders were identified via outcrossing to WT
503 fish. The transgenic F1 fish were then selected and raised. At least two independent transgenic lines
504 were initially examined and raised to confirm the equivalency of expression patterns. Only one
505 transgenic line for each stable transgenic reporter was maintained. For experiments, homozygous
506 transgenic *3'reg1:GFP* reporter fish were outcrossed to WT AB/TL fish.
507
508 **Drug treatments**
509 All drug treatments were performed on embryos beginning at the 20s stage in 2 mL of embryo
510 water with drugs at the specified concentrations in 3 mL glass vials. 30 embryos/vial were used for all
511 experiments. Treated embryos in vials were placed on a nutator in an incubator at 28.5°C for the
512 duration of the treatments. Concentrations of drugs used for treatments were: 1 μM RA (Sigma
513 R2625), 2.5 μM DEAB (Sigma-Aldrich, Cat # D86256), 5 μM BIO (Tocris, Cat # 3194), 10 μM XAV939
514 (Tocris, Cat # 3748), 75 μM CYA (Sigma-Aldrich, Cat # C4116), 10 μM SAG (Tocris, Cat # 4366). All
515 the drugs were rinsed out with blue water three times at 48 hpf prior to processing for IHC performed
516 as described below.
517
518 **Immunohistochemistry (IHC) and cardiomyocyte quantification**
519 IHC was performed as has been previously reported [18]. Briefly, embryos at the indicated
520 stages were fixed for 1 hr at RT in 1% formaldehyde/1X PBS in 3 ml glass vials. Embryos were
521 washed 1X in PBS and then 2X in 0.1% saponin/1X PBS, followed by blocking in 0.1% saponin/0.5%
522 sheep serum/1X PBS (Saponin blocking solution) for one hr. Primary antibodies were applied to the
523 embryos in blocking solution overnight at 4°C. Embryos were then gently washed 3X with 0.1%
524 saponin/1X PBS followed by 2 hr incubation with secondary antibodies at RT. Secondary antibodies
525 were washed out with 0.1% saponin/1X PBS. Primary antibodies used were: rabbit anti-Nr2f1a (1:100;
526 custom antibody [12]), rabbit anti-DsRED (1:1000; Clontech, Cat # 632496), chicken anti-GFP (1:250;
527 Invitrogen, Cat # A10262), mouse anti-Amhc (1:10, Developmental Studies Hybridoma Bank, Cat #

528 S46), mouse anti-Mhc (1:10, Developmental Studies Hybridoma Bank, Cat #, MF20). Secondary
529 antibodies used: Goat anti-mouse IgG1 DyLight (1:250, Biolegend, Cat # 409109), Goat anti-chicken
530 IgY Alexa Fluor 488 (1:500, Invitrogen, Cat # A11039), Goat anti-rabbit IgG TRITC (1:100, Southern
531 Biotech, Cat # 4050-03), Goat anti-mouse IgG2b TRITC (Southern Biotech, 1:100, Cat # 1090-03).
532 Cardiomyocytes were quantified as previously reported [46]. Briefly, embryos were mounted ventral
533 side down on coverslips. Images of the hearts were taken using a Nikon A1R Confocal Microscope
534 with a 16X water immersion objective and the resonance scanner. The number of Nr2f1a^{+} and
535 *myl7:*DsRed2-NLS^{+} nuclei in Amhc+ cardiomyocytes were counted in the images using Fiji [96].
536 Embryos were genotyped following imaging and cardiomyocyte quantification.
537
538 **In situ hybridization (ISH)**
539 Whole-mount ISH was conducted similar to what has been previously reported [18]. Briefly,
540 embryos were fixed overnight at 4°C in 4% paraformaldehyde/1X PBS in 3 ml glass vials.
541 Subsequently, embryos were rinsed with PBS/0.1% Tween-20 (PBST) 3X and then dehydrated with
542 increased percentage of methanol in PBST in series to 100% methanol and stored overnight at 4°C.
543 Embryos were then rehydrated using a PBST/methanol series to 100% PBST, and then washed 4X
544 in PBST. Digoxygenin-labeled *GFP* (ZDB-EFG-070117-2) riboprobe was used. Anti-Digoxygenin-AP,
545 Fab fragment (Millipore-Sigma, Cat # 11093274910) was used to detect the Digoxygenin-labeled
546 riboprobe in embryos. 3.5µL/mL NBT (Sigma-Roche, Cat # 11383213001) plus 3.5µL/mL BCIP
547 (Sigma-Roche, Cat # 11383221001) in the Staining buffer (0.1M Tris-HCl, pH 9.5/0.1M MgCl2/1M
548 NaCl/0.1% Tween-20) were used for the coloration reaction. Embryos were then rinsed with PBST
549 3X and dehydrated with a methanol/PBST series to 100% methanol, stored overnight at 4°C, followed
550 by rehydration using a PBST/methanol series to 100% PBST. The embryos were then put in a
551 glycerol/PBST series to 80% glycerol/PBST for imaging with a Zeiss_v12 M2Bio Stereo Microscope.
552
553 **Real Time qPCR**
554 Total RNA isolation and RT-qPCR were performed as previously described [97]. Whole
555 embryo RNA was obtained from groups of 30 24 hpf embryos using TRIzol (Invitrogen, Cat #
556 15596026) and Purelink RNA Microkit (Invitrogen, Cat # 12183016). cDNA was generated using 1µg

557 total RNA and the Superscript Reverse Transcriptase kit (Invitrogen, Cat # 18080-051). RT-qPCR for
558 *dkk1a* and *axin1*, was carried out using Power SYBR Green PCR Master Mix (Applied Biosystems,
559 Cat # 4368706) in a BioRad CFX-96 PCR machine. Expression levels were standardized to *β-actin*
560 expression [97] and data were analyzed using the Livak $2^{-\Delta\Delta CT}$ Method [98]. Each experiment was
561 performed in triplicate. Primers used are listed in **S3 Table.**
562
563 **Generation of zebrafish mutants and crispants**
564 The *3'reg1* deletion mutants and *foxf1* crispants were made using CRISPR/Cas12a (Cfp1),
565 similar to what has been reported [60]. *Acidaminococcus sp. BV3L6 (As)* crRNAs were generated to
566 the 5'- and 3'- sequences of the *3'reg1-nr2f1a* enhancer and the coding region of *foxf1* exon1 using
567 CHOPCHOP (http://chopchop.cbu.uib.no) [61]. The target-specific sequences at the 3'-end of the *As*
568 crRNAs were fused with the common portion of the *As* crRNA with a T7 site at the 5'-end using PCR.
569 The *As* crRNAs were then generated using T7 MEGAScript Kit (Thermo Fisher, Cat # AM1333). A
570 solution of 2 *As* crRNAs (380 pg/µl) were incubated at RT with *As* Cas12a protein (2 µg/µl; IDT, Cat
571 # 10001272) for 20 minutes prior to injection. 760 ng of the crRNA mixture was co-injected along with
572 4 ng of AsCas12a protein. Multiple pools of 10 embryos were screened for efficacy of the crRNA pairs
573 in generating deletions with PCR. For the *3'reg1* enhancer, sibling embryos from injections that
574 showed efficiency of the crRNAs in creating the appropriate deletions were raised to adulthood.
575 Multiple pools of F1 progeny from founders were then screened for deletions using PCR, followed by
576 cloning and sequencing. A *3'reg1* allele with a 354 bp deletion was identified and subsequently
577 recovered. For the *foxf1* crispants, the *3'reg1:GFP* reporter embryos were scored for the presence of
578 GFP and the individual embryos were screened for the efficacy of the deletions following imaging.
579 Oligos used for generation of the sgRNA are listed in **S4 Table**. Primers used for genotyping and
580 testing gRNA efficiency are listed in **S5 Table**.
581
582 **Statistical analysis**
583 To determine if two proportions were statistically distinct, we performed Fisher's exact test. To
584 determine if proportions involving more than 2 conditions were statistically different, we performed a
585 Chi-square test. To determine if the qPCR results were significant, we performed a Student's t-test

586 with Welch's correction. To compare 3 or more distinct conditions (cell quantification), we performed
587 an ordinary one-way ANOVA with multiple comparisons. Statistical analyses were performed utilizing
588 GraphPad Prism. A p value <0.05 was considered statistically significant for all analysis.

589 **Figure Legends**

590 **Figure 1. The *3'reg1-nr2f1a* enhancer is expressed in the atrium. A)** ATAC-seq profiling from ACs
591 showing regions of open chromatin near the *nr2f1a* locus (purple). Black bars indicate called regions
592 of open chromatin. Black box indicates *3'reg1*. **B)** VISTA plot showing conservation of zebrafish
593 *3'reg1* enhancer in *Callorhincus milli* (Australian ghostshark), *Xenopus tropicalis* (Tropical clawed
594 frog), *Anolis carolinensis* (Green Anole), *Mus musculus* (House mouse), and *Homo sapiens* (human).
595 Pink indicates >50% conservation of regulatory regions with zebrafish *3'reg1*. Median lines in
596 individual VISTA plots indicate 75% conservation. **C)** Clustal alignment of *3'reg1* from the VISTA plot
597 in indicated species. Black asterisks indicate conserved nucleotides. Red asterisks indicate partially
598 conserved nucleotides. Conserved putative binding sites for Foxf (blue shade) and Lef/Tcf (purple
599 shade) TFs. **D)** Schematic of the *3'reg1:GFP* reporter vector. **E)** *In situ* hybridization (ISH) for *gfp* in
600 transgenic *3'reg1:GFP* embryo at 24 hpf (n=24). Venous pole of the heart tube (black arrowhead).
601 View is lateral with anterior left and dorsal up. Scale bar: 200μm. **F-H)** Confocal images of hearts from
602 transgenic *3'reg1:GFP* embryos stained for *3'reg1*:GFP (green), Vmhc (VCs – red), and Amhc (ACs
603 – blue). 36 hpf (n=5), 48 hpf (n=7), 72 hpf (n=5). *3'reg1:GFP* in the atria of the hearts (white
604 arrowhead). Images are frontal views with the arterial pole up. n indicates the number of embryos
605 examined for a representative experiment. Scale bar: 50 μm. **** indicate P < 0.0001.

606

607 **Figure 2. Tcf7l1a restricts *3'reg1* reporter expression within the heart. A)** Schematics of
608 *3'reg1:GFP* reporter constructs. Foxf sites (blue), Lef/Tcf site (purple), mutated Lef/Tcf site (red), and
609 deleted Lef/Tcf site (black). **B)** Sequences of the WT (purple), mutated (red), and deleted Left/Tcf
610 sites within the *3'reg1* enhancer. **C-E)** Confocal images of hearts from embryos injected with the
611 *3'reg1:GFP*, *3'reg1-mTcf:GFP*, *3'reg1-ΔTcf:GFP* constructs. **F)** The percentage of transient
612 transgenic embryos with reporter atrial, pan-cardiac, and lacking expression in their hearts.
613 *3'reg1:GFP* (n=200); *3'reg1-mTcf:GFP* (n=101); *3'reg1-ΔTcf:GFP* (n=102). **G,H)** Confocal images of
614 hearts from control and *tcf7l1a* MO-injected transgenic *3'reg1:GFP* embryos. **I)** The percentage of
615 stable *3'reg1:GFP* embryos with reporter atrial and pan-cardiac expression in their hearts. Control
616 (n=152); *tcf7l1a-MO* (n=92). Images are frontal views with the arterial pole up. Hearts are stained for
617 *3'reg1*:GFP (green), Vmhc (red), Amhc (blue). Scale bars: 50 μm. **** indicate P < 0.0001.

618

619 **Figure 3. Wnt signaling promotes *3'reg1* reporter expression and AC differentiation. A-C)**
620 Confocal images of hearts from control, BIO-, and XAV-treated *3'reg1:GFP* embryos stained for
621 *3'reg1*:GFP (green), Vmhc (red), Amhc (blue). **D)** The percentage of control and treated *3'reg1:*GFP
622 embryos with atrial, pan-cardiac, and lacking expression in their hearts. Control (n=35); BIO (n=32);
623 XAV (n=49). **E-G)** Confocal images of hearts from control, BIO-, and XAV-treated embryos stained
624 for Nr2f1a (green), Mhc (pan-cardiac, red), Amhc (blue). **H)** The number of Nr2f1a$^+$/Amhc$^+$
625 cardiomyocytes with the hearts of control, BIO-, and XAV-treated embryos. Control (n=12); BIO
626 (n=11); XAV (n=11). **I-K)** Confocal images of hearts from control, BIO-, and XAV-treated
627 *myl7:DsRed2-NLS* (*myl7:DRN*) embryos stained for DsRed-NLS (pan-cardiac nuclei - red) and Amhc
628 (blue). **L)** The number of *myl7:*DsRed2-NLS$^+$/Amhc$^+$ cardiomyocytes (ACs) within the hearts of
629 control, BIO-, and XAV-treated *myl7:DsRed2-NLS* embryos. Control (n=9); BIO (n=10); XAV (n=8).
630 Scale bars: 50 μm. Error bars in graphs indicate s.e.m.. *** indicate P < 0.001. **** indicate P < 0.0001.

631

632 **Figure 4. Foxf1 promotes *3'reg1* reporter expression within the heart. A)** Schematics of
633 *3'reg1:GFP* reporter constructs with WT, deleted, and mutated Foxf sites. Foxf sites (blue), mutated
634 Foxf sites (red), deleted Foxf sites (black), and Lef/Tcf site (purple). **B)** Sequences of the WT (blue),
635 mutated (red), and deleted (dashes) Foxf sites within the *3'reg1* enhancer. **C)** The percentage of
636 transient transgenic embryos with reporter expression in the atria. Control (*3'reg1*) (n=150); *mFoxf-A*
637 (n=60); Δ*Foxf-A* (n=101); *mFoxf-B* (n=49); Δ*Foxf-B* (n=200); *mFoxf-C* (n=98); Δ*Foxf-C* (n=195). **D-F)**
638 Confocal images of hearts from control uninjected, *Foxf1* mRNA and *dnFoxf1* mRNA injected
639 *3'reg1:GFP* embryos stained for *3'reg1*:GFP (green), Vmhc (red), Amhc (blue). **G)** The percentage of
640 injected *3'reg1:GFP* embryos with atrial expression, pan-cardiac expression, and lacking expression.
641 Control (n=35); *Foxf1* (n=29); *dnFoxf1* (n=59). **H-J)** Confocal images of hearts from control, *Foxf1*
642 mRNA, and *dnFoxf1* mRNA injected embryos stained for Nr2f1a (green), Mhc (red), Amhc (blue). **K)**
643 The number of Nr2f1a$^+$/Amhc$^+$ cardiomyocytes (ACs) within the hearts of control, *Foxf1* mRNA, and
644 *dnFoxf1* injected embryos. Control (n=8); *Foxf1* (n=11); *dnFoxf1* (n=8). **L-N)** Confocal images of
645 hearts from control, *Foxf1* mRNA, and *dnFoxf1* injected *myl7:DsRed2-NLS* (*myl7:DRN*) embryos
646 stained for DsRed-NLS (red) and Amhc (blue). **O)** Quantification of the number of *myl7:*DsRed2-

647 NLS$^+$/Amhc$^+$ cardiomyocytes (ACs) within the hearts of control, *Foxf1* mRNA, and *dnFoxf1* injected
648 *myl7:DsRed2-NLS* embryos. Control (n=10); *Foxf1* (n=13); *dnFoxf1* (n=11). Scale bars: 50 μm. Error
649 bars in graphs indicate s.e.m.. *** indicate P < 0.001. **** indicate P < 0.0001.
650
651 **Figure 5. Tcf7l1a limits the ability of Foxf1 to promote *3'reg1* reporter expression. A-D)** Confocal
652 images of hearts from control, *Foxf1* mRNA injected, XAV-treated, and *Foxf1* mRNA injected plus
653 XAV-treated *3'reg1:GFP* embryos . **E)** The percentage of control, *Foxf1* mRNA injected, XAV-treated,
654 and *Foxf1* mRNA injected plus XAV-treated *3'reg1:GFP* embryos with atrial expression, pan-cardiac
655 expression, and lacking expression. Control (n=26); *Foxf1* (n=24); XAV n=98; *Foxf1*-XAV (n=103). **F-**
656 **I)** Confocal images of hearts from control, *Foxf1* mRNA injected, *tcf7l1a* mRNA injected, and *Foxf1*
657 mRNA and t*cf7l1a* mRNA co-injected *3'reg1:GFP* embryos. **E)** The percentage of control, *Foxf1*
658 mRNA injected, *tcf7l1a* mRNA injected, and *Foxf1* mRNA and t*cf7l1a* mRNA co-injected *3'reg1:GFP*
659 embryos with atrial expression, pan-cardiac expression, and lacking expression. Control (n=39),
660 *Foxf1* (n=34); *tcf7l1a* (n=95); *Foxf1-tcf7l1a* (n=51). **K-N)** Confocal images of hearts from control,
661 *dnFoxf1* mRNA injected, *tcf7l1a* MO injected, and *Foxf1* mRNA and t*cf7l1a* MO co-injected
662 *3'reg1:GFP* embryos. **O)** The percentage of control, *dnFoxf1* mRNA injected, *tcf7l1a* MO injected,
663 and *Foxf1* mRNA and t*cf7l1a* MO *3'reg1:*GFP embryos with atrial expression, pan-cardiac expression,
664 and lacking expression. Control (n=27), *dnFoxf1* (n=102); *Tcf7l1a-MO* (n=96); *dnFoxf1-tcf7l1aMO*
665 (n=100). Hearts are stained for *3'reg1*:GFP (green), Vmhc (red), Amhc (blue)Scale bars: 50 μm. ****
666 indicate P < 0.0001.
667
668 **Figure 6. Wnt signaling and Foxf1 require Nr2f1a to promote a surplus of cardiomyocytes. A-**
669 **D)** Confocal images of hearts from untreated and BIO-treated WT and *nr2f1a$^{-/-}$ myl7:DsRed2-NLS*
670 embryos. **E)** The number of *myl7:*DsRed2-NLS$^+$/Amhc$^+$ cardiomyocytes in hearts of untreated and
671 BIO-treated WT and *nr2f1a$^{-/-}$ myl7:DsRed2-NLS* embryos. Untreated WT (n=12); untreated *nr2f1a$^{-/-}$*
672 (n=7); treated WT (n=11); treated *nr2f1a$^{-/-}$* (n= 10). **F-I)** Confocal images of hearts from uninjected
673 and *Foxf1* mRNA-injected WT and *nr2f1a$^{-/-}$ myl7:DsRed2-NLS* embryos. **J)** The number of
674 *myl7:*DsRed2-NLS$^+$/Amhc$^+$ cardiomyocytes in uninjected and *Foxf1* mRNA-injected WT and *nr2f1a$^{-/-}$*
675 *myl7:DsRed2-NLS* embryos. Uninjected WT (n=7); Uninjected *nr2f1a$^{-/-}$* (n=5); Inj. WT (n=10); Injected

676 *nr2f1a*$^{-/-}$ (n=5). Hearts are stained for DsRed-NLS (red) and Amhc (blue). Scale bars: 50 μm. Error
677 bars in graphs indicate s.e.m.. ** indicate P < 0.01. **** indicate P < 0.001. **** indicate P < 0.0001.
678 ns indicates not a statistically significant difference.
679
680 **Figure 7. Wnt signaling and Foxf1 require 3*'reg1* to promote a surplus ACs. A)** Schematic of
681 *3'reg1* enhancer deletion generated using CRISPR/Cas12a. Arrows indicate location of the guides.
682 **B-E)** Confocal images of hearts from untreated and BIO-treated WT and *3'reg1*$^{\Delta/\Delta}$ embryos stained
683 for Nr2f1a (green), Mhc (red), and Amhc (blue). BIO was unable to promote an increase in ACs in
684 *3'reg1*$^{-/-}$ embryos. **E)** The number of Nr2f1a^{+}/Amhc^{+} cardiomyocytes in untreated and BIO-treated WT
685 and *3'reg1*$^{-/-}$ embryos. Untreated WT (n=9); untreated *3'reg1*$^{-/-}$ (n=5); treated WT (n=11); treated
686 *3'reg1*$^{-/-}$ (n=4). **F-I)** Confocal images of hearts from uninjected and *Foxf1* mRNA-injected WT and
687 *3'reg1*$^{-/-}$ embryos stained for Nr2f1a (green), Mhc (red), and Amhc (blue). **J)** The number of
688 Nr2f1a^{+}/Amhc^{+} cardiomyocytes in uninjected and *Foxf1* mRNA-injected WT and Nr2f1a^{+} *3'reg1*$^{-/-}$
689 embryos. Uninjected WT (n=11); Uninjected *3'reg1*$^{-/-}$ (n=4); Injected WT (n=12); Injected *3'reg1*$^{-/-}$ (n=
690 4). Scale bar: 50 μm. Error bars in graphs indicate s.e.m.. **** indicate P < 0.0001. ns indicates not a
691 statistically significant difference.
692
693 **Figure 8. A Wnt-Foxf1-Nr2f1a cascade directs atrial cardiomyocyte differentiation.** Model
694 depicting the Wnt signaling and Foxf1-dependent regulatory network that controls Nr2f1a expression
695 and the role of the *3'reg1* enhancer in the atrial cardiomyocyte differentiation during early heart tube
696 development.
697

698 **References**

699 1. Targoff KL, Colombo S, George V, Schell T, Kim S-H, Solnica-Krezel L, et al. Nkx genes are
700 essential for maintenance of ventricular identity. Development. 2013;140: 4203–4213.
701 doi:10.1242/dev.095562

702 2. van Weerd JH, Christoffels VM. The formation and function of the cardiac conduction system.
703 Development. 2016;143: 197–210. doi:10.1242/dev.124883

704 3. Bruneau BG, Riley P. Heart Development and Disease. Cold Spring Harbor Laboratory Press;
705 2020. Available: https://play.google.com/store/books/details?id=pwE6yAEACAAJ

706 4. Pereira FA, Qiu Y, Zhou G, Tsai M-J, Tsai SY. The orphan nuclear receptor COUP-TFII is
707 required for angiogenesis and heart development. Genes & Development. 1999. pp. 1037–1049.
708 doi:10.1101/gad.13.8.1037

709 5. Devalla HD, Schwach V, Ford JW, Milnes JT, El-Haou S, Jackson C, et al. Atrial-like
710 cardiomyocytes from human pluripotent stem cells are a robust preclinical model for assessing
711 atrial-selective pharmacology. EMBO Mol Med. 2015;7: 394–410.
712 doi:10.15252/emmm.201404757

713 6. Li G, Xu A, Sim S, Priest JR, Tian X, Khan T, et al. Transcriptomic Profiling Maps Anatomically
714 Patterned Subpopulations among Single Embryonic Cardiac Cells. Dev Cell. 2016;39: 491–507.
715 doi:10.1016/j.devcel.2016.10.014

716 7. Al Turki S, Manickaraj AK, Mercer CL, Gerety SS, Hitz M-P, Lindsay S, et al. Rare variants in
717 NR2F2 cause congenital heart defects in humans. Am J Hum Genet. 2014;94: 574–585.
718 doi:10.1016/j.ajhg.2014.03.007

719 8. Schott JJ, Benson DW, Basson CT, Pease W, Silberbach GM, Moak JP, et al. Congenital heart
720 disease caused by mutations in the transcription factor NKX2-5. Science. 1998;281: 108–111.
721 doi:10.1126/science.281.5373.108

722 9. Nakamura E, Makita Y, Okamoto T, Nagaya K, Hayashi T, Sugimoto M, et al. 5.78 Mb terminal

723 deletion of chromosome 15q in a girl, evaluation of NR2F2 as candidate gene for congenital heart
724 defects. Eur J Med Genet. 2011;54: 354–356. doi:10.1016/j.ejmg.2010.12.004

725 10. Ahmed I, Anjum F. Atrioventricular Septal Defect. StatPearls. Treasure Island (FL): StatPearls
726 Publishing; 2023. Available: https://www.ncbi.nlm.nih.gov/pubmed/32965865

727 11. Wu S-P, Cheng C-M, Lanz RB, Wang T, Respress JL, Ather S, et al. Atrial identity is determined
728 by a COUP-TFII regulatory network. Dev Cell. 2013;25: 417–426.
729 doi:10.1016/j.devcel.2013.04.017

730 12. Duong TB, Ravisankar P, Song YC, Gafranek JT, Rydeen AB, Dohn TE, et al. Nr2f1a balances
731 atrial chamber and atrioventricular canal size via BMP signaling-independent and -dependent
732 mechanisms. Dev Biol. 2018;434: 7–14. doi:10.1016/j.ydbio.2017.11.010

733 13. Dohn TE, Ravisankar P, Tirera FT, Martin KE, Gafranek JT, Duong TB, et al. Nr2f-dependent
734 allocation of ventricular cardiomyocyte and pharyngeal muscle progenitors. PLoS Genet.
735 2019;15: e1007962. doi:10.1371/journal.pgen.1007962

736 14. Xie X, Qin J, Lin S-H, Tsai SY, Tsai M-J. Nuclear receptor chicken ovalbumin upstream promoter-
737 transcription factor II (COUP-TFII) modulates mesenchymal cell commitment and differentiation.
738 Proc Natl Acad Sci U S A. 2011;108: 14843–14848. doi:10.1073/pnas.1110236108

739 15. Niederreither K, Subbarayan V, Dollé P, Chambon P. Embryonic retinoic acid synthesis is
740 essential for early mouse post-implantation development. Nat Genet. 1999;21: 444–448.
741 doi:10.1038/7788

742 16. Niederreither K, Vermot J, Messaddeq N, Schuhbaur B, Chambon P, Dollé P. Embryonic retinoic
743 acid synthesis is essential for heart morphogenesis in the mouse. Development. 2001;128:
744 1019–1031. doi:10.1242/dev.128.7.1019

745 17. Ryckebusch L, Wang Z, Bertrand N, Lin S-C, Chi X, Schwartz R, et al. Retinoic acid deficiency
746 alters second heart field formation. Proc Natl Acad Sci U S A. 2008;105: 2913–2918.
747 doi:10.1073/pnas.0712344105

748 18. Duong TB, Holowiecki A, Waxman JS. Retinoic acid signaling restricts the size of the first heart
749 field within the anterior lateral plate mesoderm. Dev Biol. 2021;473: 119–129.
750 doi:10.1016/j.ydbio.2021.02.005

751 19. Pereira FA, Tsai MJ, Tsai SY. COUP-TF orphan nuclear receptors in development and
752 differentiation. Cell Mol Life Sci. 2000;57: 1388–1398. doi:10.1007/PL00000624

753 20. Lin F-J, Qin J, Tang K, Tsai SY, Tsai M-J. Coup d'Etat: an orphan takes control. Endocr Rev.
754 2011;32: 404–421. doi:10.1210/er.2010-0021

755 21. Love CE, Prince VE. Expression and retinoic acid regulation of the zebrafish nr2f orphan nuclear
756 receptor genes. Dev Dyn. 2012;241: 1603–1615. doi:10.1002/dvdy.23838

757 22. Laursen KB, Mongan NP, Zhuang Y, Ng MM, Benoit YD, Gudas LJ. Polycomb recruitment
758 attenuates retinoic acid–induced transcription of the bivalent NR2F1 gene. Nucleic Acids Res.
759 2013;41: 6430–6443. doi:10.1093/nar/gkt367

760 23. Lee JH, Protze SI, Laksman Z, Backx PH, Keller GM. Human Pluripotent Stem Cell-Derived Atrial
761 and Ventricular Cardiomyocytes Develop from Distinct Mesoderm Populations. Cell Stem Cell.
762 2017;21: 179–194.e4. doi:10.1016/j.stem.2017.07.003

763 24. Lemme M, Ulmer BM, Lemoine MD, Zech ATL, Flenner F, Ravens U, et al. Atrial-like Engineered
764 Heart Tissue: An In Vitro Model of the Human Atrium. Stem Cell Reports. 2018;11: 1378–1390.
765 doi:10.1016/j.stemcr.2018.10.008

766 25. Wiesinger A, Boink GJJ, Christoffels VM, Devalla HD. Retinoic acid signaling in heart
767 development: Application in the differentiation of cardiovascular lineages from human pluripotent
768 stem cells. Stem Cell Reports. 2021;16: 2589–2606. doi:10.1016/j.stemcr.2021.09.010

769 26. D'Aniello E, Waxman JS. Input overload: Contributions of retinoic acid signaling feedback
770 mechanisms to heart development and teratogenesis. Dev Dyn. 2015;244: 513–523.
771 doi:10.1002/dvdy.24232

772 27. Quaranta R, Fell J, Rühle F, Rao J, Piccini I, Araúzo-Bravo MJ, et al. Revised roles of ISL1 in a

773 hES cell-based model of human heart chamber specification. Elife. 2018;7.
774 doi:10.7554/eLife.31706

775 28. Boogerd CJ, Zhu X, Aneas I, Sakabe N, Zhang L, Sobreira DR, et al. Tbx20 Is Required in Mid-
776 Gestation Cardiomyocytes and Plays a Central Role in Atrial Development. Circ Res. 2018;123:
777 428–442. doi:10.1161/CIRCRESAHA.118.311339

778 29. Krishnan V, Pereira FA, Qiu Y, Chen CH, Beachy PA, Tsai SY, et al. Mediation of Sonic
779 hedgehog-induced expression of COUP-TFII by a protein phosphatase. Science. 1997;278:
780 1947–1950. doi:10.1126/science.278.5345.1947

781 30. Hoffmann AD, Yang XH, Burnicka-Turek O, Bosman JD, Ren X, Steimle JD, et al. Foxf genes
782 integrate tbx5 and hedgehog pathways in the second heart field for cardiac septation. PLoS
783 Genet. 2014;10: e1004604. doi:10.1371/journal.pgen.1004604

784 31. Xie L, Hoffmann AD, Burnicka-Turek O, Friedland-Little JM, Zhang K, Moskowitz IP. Tbx5-
785 hedgehog molecular networks are essential in the second heart field for atrial septation. Dev Cell.
786 2012;23: 280–291. doi:10.1016/j.devcel.2012.06.006

787 32. Steimle JD, Rankin SA, Slagle CE, Bekeny J, Rydeen AB, Chan SS-K, et al. Evolutionarily
788 conserved Tbx5-Wnt2/2b pathway orchestrates cardiopulmonary development. Proc Natl Acad
789 Sci U S A. 2018;115: E10615–E10624. doi:10.1073/pnas.1811624115

790 33. Briggs LE, Burns TA, Lockhart MM, Phelps AL, Van den Hoff MJB, Wessels A. Wnt/β-catenin
791 and sonic hedgehog pathways interact in the regulation of the development of the dorsal
792 mesenchymal protrusion. Dev Dyn. 2016;245: 103–113. doi:10.1002/dvdy.24339

793 34. Hong N, Zhang E, Xie H, Jin L, Zhang Q, Lu Y, et al. The transcription factor Sox7 modulates
794 endocardiac cushion formation contributed to atrioventricular septal defect through Wnt4/Bmp2
795 signaling. Cell Death Dis. 2021;12: 393. doi:10.1038/s41419-021-03658-z

796 35. Martin KE, Ravisankar P, Beerens M, MacRae CA, Waxman JS. Nr2f1a maintains atrial nkx2.5
797 expression to repress pacemaker identity within venous atrial cardiomyocytes of zebrafish. Elife.
798 2023;12. doi:10.7554/eLife.77408

799 36. Zabidi MA, Stark A. Regulatory Enhancer-Core-Promoter Communication via Transcription
800 Factors and Cofactors. Trends Genet. 2016;32: 801–814. doi:10.1016/j.tig.2016.10.003

801 37. Coppola U, Waxman JS. Origin and evolutionary landscape of Nr2f transcription factors across
802 Metazoa. PLoS One. 2021;16: e0254282. doi:10.1371/journal.pone.0254282

803 38. Birnbaum RY, Clowney EJ, Agamy O, Kim MJ, Zhao J, Yamanaka T, et al. Coding exons function
804 as tissue-specific enhancers of nearby genes. Genome Res. 2012;22: 1059–1068. Available:
805 https://genome.cshlp.org/content/22/6/1059.short

806 39. Bradford YM, Van Slyke CE, Ruzicka L, Singer A, Eagle A, Fashena D, et al. Zebrafish
807 information network, the knowledgebase for Danio rerio research. Genetics. 2022;220.
808 doi:10.1093/genetics/iyac016

809 40. Weirauch MT, Yang A, Albu M, Cote AG, Montenegro-Montero A, Drewe P, et al. Determination
810 and inference of eukaryotic transcription factor sequence specificity. Cell. 2014;158: 1431–1443.
811 doi:10.1016/j.cell.2014.08.009

812 41. Lambert SA, Yang AWH, Sasse A, Cowley G, Albu M, Caddick MX, et al. Similarity regression
813 predicts evolution of transcription factor sequence specificity. Nat Genet. 2019;51: 981–989.
814 doi:10.1038/s41588-019-0411-1

815 42. Gupta S, Stamatoyannopoulos JA, Bailey TL, Noble WS. Quantifying similarity between motifs.
816 Genome Biol. 2007;8: R24. doi:10.1186/gb-2007-8-2-r24

817 43. Bailey TL, Boden M, Buske FA, Frith M, Grant CE, Clementi L, et al. MEME SUITE: tools for
818 motif discovery and searching. Nucleic Acids Res. 2009;37: W202–8. doi:10.1093/nar/gkp335

819 44. Castro-Mondragon JA, Riudavets-Puig R, Rauluseviciute I, Lemma RB, Turchi L, Blanc-Mathieu
820 R, et al. JASPAR 2022: the 9th release of the open-access database of transcription factor
821 binding profiles. Nucleic Acids Res. 2022;50: D165–D173. doi:10.1093/nar/gkab1113

822 45. Niederreither K, Dollé P. Retinoic acid in development: towards an integrated view. Nat Rev
823 Genet. 2008;9: 541–553. doi:10.1038/nrg2340

824 46. Song YC, Dohn TE, Rydeen AB, Nechiporuk AV, Waxman JS. HDAC1-mediated repression of
825 the retinoic acid-responsive gene ripply3 promotes second heart field development. PLoS Genet.
826 2019;15: e1008165. doi:10.1371/journal.pgen.1008165

827 47. Cadigan KM, Waterman ML. TCF/LEFs and Wnt signaling in the nucleus. Cold Spring Harb
828 Perspect Biol. 2012;4. doi:10.1101/cshperspect.a007906

829 48. Wang Z, Li Z, Ji H. Direct targeting of β-catenin in the Wnt signaling pathway: Current progress
830 and perspectives. Med Res Rev. 2021;41: 2109–2129. doi:10.1002/med.21787

831 49. Liang W, Han P, Kim EH, Mak J, Zhang R, Torrente AG, et al. Canonical Wnt signaling promotes
832 pacemaker cell specification of cardiac mesodermal cells derived from mouse and human
833 embryonic stem cells. Stem Cells. 2020;38: 352–368. doi:10.1002/stem.3106

834 50. Willems L, Daniëls A, Fanton Y, Linsen L, Evens L, Bito V, et al. Differentiation of Human Cardiac
835 Atrial Appendage Stem Cells into Adult Cardiomyocytes: A Role for the Wnt Pathway? Int J Mol
836 Sci. 2020;21. doi:10.3390/ijms21113931

837 51. Dohn TE, Waxman JS. Distinct phases of Wnt/β-catenin signaling direct cardiomyocyte formation
838 in zebrafish. Dev Biol. 2012;361: 364–376. doi:10.1016/j.ydbio.2011.10.032

839 52. Ueno S, Weidinger G, Osugi T, Kohn AD, Golob JL, Pabon L, et al. Biphasic role for Wnt/β-
840 catenin signaling in cardiac specification in zebrafish and embryonic stem cells. Proceedings of
841 the National Academy of Sciences. 2007;104: 9685–9690. doi:10.1073/pnas.0702859104

842 53. Sorrell MRJ, Dohn TE, D'Aniello E, Waxman JS. Tcf7l1 proteins cell autonomously restrict
843 cardiomyocyte and promote endothelial specification in zebrafish. Dev Biol. 2013;380: 199–210.
844 doi:10.1016/j.ydbio.2013.05.016

845 54. Dorsky RI, Itoh M, Moon RT, Chitnis A. Two tcf3 genes cooperate to pattern the zebrafish brain.
846 Development. 2003;130: 1937–1947. doi:10.1242/dev.00402

847 55. Thomas NA, Koudijs M, van Eeden FJM, Joyner AL, Yelon D. Hedgehog signaling plays a cell-
848 autonomous role in maximizing cardiac developmental potential. Development. 2008;135: 3789–

849 3799. doi:10.1242/dev.024083

850 56. Telias M, Ben-Yosef D. Pharmacological Manipulation of Wnt/β-Catenin Signaling Pathway in
851 Human Neural Precursor Cells Alters Their Differentiation Potential and Neuronal Yield. Front
852 Mol Neurosci. 2021;14: 680018. doi:10.3389/fnmol.2021.680018

853 57. Mably JD, Mohideen MAPK, Burns CG, Chen J-N, Fishman MC. heart of glass regulates the
854 concentric growth of the heart in zebrafish. Curr Biol. 2003;13: 2138–2147.
855 doi:10.1016/j.cub.2003.11.055

856 58. Ormestad M, Astorga J, Carlsson P. Differences in the embryonic expression patterns of mouse
857 Foxf1 and -2 match their distinct mutant phenotypes. Dev Dyn. 2004;229: 328–333.
858 doi:10.1002/dvdy.10426

859 59. Xu P, Balczerski B, Ciozda A, Louie K, Oralova V, Huysseune A, et al. Fox proteins are modular
860 competency factors for facial cartilage and tooth specification. Development. 2018;145.
861 doi:10.1242/dev.165498

862 60. Moreno-Mateos MA, Fernandez JP, Rouet R, Vejnar CE, Lane MA, Mis E, et al. CRISPR-Cpf1
863 mediates efficient homology-directed repair and temperature-controlled genome editing. Nat
864 Commun. 2017;8: 2024. doi:10.1038/s41467-017-01836-2

865 61. Liu G, Zhang Y, Zhang T. Computational approaches for effective CRISPR guide RNA design
866 and evaluation. Comput Struct Biotechnol J. 2020;18: 35–44. doi:10.1016/j.csbj.2019.11.006

867 62. Paul B, Montoya G. CRISPR-Cas12a: Functional overview and applications. Biomed J. 2020;43:
868 8–17. doi:10.1016/j.bj.2019.10.005

869 63. Bräutigam C, Raggioli A, Winter J. The Wnt/β-catenin pathway regulates the expression of the
870 miR-302 cluster in mouse ESCs and P19 cells. PLoS One. 2013;8: e75315.
871 doi:10.1371/journal.pone.0075315

872 64. Che J, Zhang F, Zhao C, Hu X, Fan S. Cyclopamine is a novel Hedgehog signaling inhibitor with
873 significant anti-proliferative, anti-invasive and anti-estrogenic potency in human breast cancer

874 cells. Oncol Lett. 2013;5: 1417–1421. doi:10.3892/ol.2013.1195

875 65. Rimkus TK, Carpenter RL, Qasem S, Chan M, Lo H-W. Targeting the Sonic Hedgehog Signaling
876 Pathway: Review of Smoothened and GLI Inhibitors. Cancers . 2016;8.
877 doi:10.3390/cancers8020022

878 66. Hoffmann AD, Peterson MA, Friedland-Little JM, Anderson SA, Moskowitz IP. sonic hedgehog
879 is required in pulmonary endoderm for atrial septation. Development. 2009;136: 1761–1770.
880 doi:10.1242/dev.034157

881 67. Liu J, Xiao Q, Xiao J, Niu C, Li Y, Zhang X, et al. Wnt/β-catenin signalling: function, biological
882 mechanisms, and therapeutic opportunities. Signal Transduct Target Ther. 2022;7: 3.
883 doi:10.1038/s41392-021-00762-6

884 68. Liu K, Petree C, Requena T, Varshney P, Varshney GK. Expanding the CRISPR Toolbox in
885 Zebrafish for Studying Development and Disease. Front Cell Dev Biol. 2019;7: 13.
886 doi:10.3389/fcell.2019.00013

887 69. Rankin SA, Steimle JD, Yang XH, Rydeen AB, Agarwal K, Chaturvedi P, et al. Tbx5 drives
888 Aldh1a2 expression to regulate a RA-Hedgehog-Wnt gene regulatory network coordinating
889 cardiopulmonary development. Elife. 2021;10. doi:10.7554/eLife.69288

890 70. Lazic S, Scott IC. Mef2cb regulates late myocardial cell addition from a second heart field-like
891 population of progenitors in zebrafish. Dev Biol. 2011;354: 123–133.
892 doi:10.1016/j.ydbio.2011.03.028

893 71. Ren J, Han P, Ma X, Farah EN, Bloomekatz J, Zeng X-XI, et al. Canonical Wnt5b Signaling
894 Directs Outlying Nkx2.5+ Mesoderm into Pacemaker Cardiomyocytes. Dev Cell. 2019;50: 729–
895 743.e5. doi:10.1016/j.devcel.2019.07.014

896 72. Kalinichenko VV, Gusarova GA, Kim I-M, Shin B, Yoder HM, Clark J, et al. Foxf1
897 haploinsufficiency reduces Notch-2 signaling during mouse lung development. Am J Physiol
898 Lung Cell Mol Physiol. 2004;286: L521–30. doi:10.1152/ajplung.00212.2003

899 73. Ustiyan V, Bolte C, Zhang Y, Han L, Xu Y, Yutzey KE, et al. FOXF1 transcription factor promotes
900 lung morphogenesis by inducing cellular proliferation in fetal lung mesenchyme. Dev Biol.
901 2018;443: 50–63. doi:10.1016/j.ydbio.2018.08.011

902 74. Askary A, Xu P, Barske L, Bay M, Bump P, Balczerski B, et al. Genome-wide analysis of facial
903 skeletal regionalization in zebrafish. Development. 2017;144: 2994–3005.
904 doi:10.1242/dev.151712

905 75. Shen G, Ren H, Shang Q, Zhao W, Zhang Z, Yu X, et al. Foxf1 knockdown promotes BMSC
906 osteogenesis in part by activating the Wnt/β-catenin signalling pathway and prevents
907 ovariectomy-induced bone loss. EBioMedicine. 2020;52: 102626.
908 doi:10.1016/j.ebiom.2020.102626

909 76. Ji W, Sun X. Methyl-CpG-binding protein 2 promotes osteogenic differentiation of bone marrow
910 mesenchymal stem cells through regulating forkhead box F1/Wnt/β-Catenin axis. Bioengineered.
911 2022;13: 583–592. doi:10.1080/21655979.2021.2012357

912 77. Koch S. Regulation of Wnt Signaling by FOX Transcription Factors in Cancer. Cancers . 2021;13.
913 doi:10.3390/cancers13143446

914 78. Zaret KS, Carroll JS. Pioneer transcription factors: establishing competence for gene expression.
915 Genes Dev. 2011;25: 2227–2241. doi:10.1101/gad.176826.111

916 79. Iwafuchi-Doi M, Donahue G, Kakumanu A, Watts JA, Mahony S, Pugh BF, et al. The Pioneer
917 Transcription Factor FoxA Maintains an Accessible Nucleosome Configuration at Enhancers for
918 Tissue-Specific Gene Activation. Mol Cell. 2016;62: 79–91. doi:10.1016/j.molcel.2016.03.001

919 80. Wang S, Yan S, Zhu S, Zhao Y, Yan J, Xiao Z, et al. FOXF1 Induces Epithelial-Mesenchymal
920 Transition in Colorectal Cancer Metastasis by Transcriptionally Activating SNAI1. Neoplasia.
921 2018;20: 996–1007. doi:10.1016/j.neo.2018.08.004

922 81. Lo P-K, Lee JS, Liang X, Han L, Mori T, Fackler MJ, et al. Epigenetic inactivation of the potential
923 tumor suppressor gene FOXF1 in breast cancer. Cancer Res. 2010;70: 6047–6058.
924 doi:10.1158/0008-5472.CAN-10-1576

925 82. Wu C-Y, Chan C-H, Dubey NK, Wei H-J, Lu J-H, Chang C-C, et al. Highly Expressed FOXF1
926 Inhibit Non-Small-Cell Lung Cancer Growth via Inducing Tumor Suppressor and G1-Phase Cell-
927 Cycle Arrest. Int J Mol Sci. 2020;21. doi:10.3390/ijms21093227

928 83. Rowton M, Perez-Cervantes C, Hur S, Jacobs-Li J, Lu E, Deng N, et al. Hedgehog signaling
929 activates a mammalian heterochronic gene regulatory network controlling differentiation timing
930 across lineages. Dev Cell. 2022;57: 2181–2203.e9. doi:10.1016/j.devcel.2022.08.009

931 84. Pi-Roig A, Martin-Blanco E, Minguillon C. Distinct tissue-specific requirements for the zebrafish
932 tbx5 genes during heart, retina and pectoral fin development. Open Biol. 2014;4: 140014.
933 doi:10.1098/rsob.140014

934 85. Boyle Anderson EAT, Ho RK. A transcriptomics analysis of the Tbx5 paralogues in zebrafish.
935 PLoS One. 2018;13: e0208766. doi:10.1371/journal.pone.0208766

936 86. Boyle-Anderson EAT, Mao Q, Ho RK. Tbx5a and Tbx5b paralogues act in combination to control
937 separate vectors of migration in the fin field of zebrafish. Dev Biol. 2022;481: 201–214.
938 doi:10.1016/j.ydbio.2021.10.008

939 87. Blow MJ, McCulley DJ, Li Z, Zhang T, Akiyama JA, Holt A, et al. ChIP-Seq identification of weakly
940 conserved heart enhancers. Nat Genet. 2010;42: 806–810. doi:10.1038/ng.650

941 88. Cannavò E, Khoueiry P, Garfield DA, Geeleher P, Zichner T, Gustafson EH, et al. Shadow
942 Enhancers Are Pervasive Features of Developmental Regulatory Networks. Curr Biol. 2016;26:
943 38–51. doi:10.1016/j.cub.2015.11.034

944 89. Westerfield M. The Zebrafish Book; A guide for the laboratory use of zebrafish (Danio rerio). (No
945 Title). 2007 [cited 9 Jan 2024]. Available: https://cir.nii.ac.jp/crid/1370283694361132063

946 90. Huang C-J, Tu C-T, Hsiao C-D, Hsieh F-J, Tsai H-J. Germ-line transmission of a myocardium-
947 specific GFP transgene reveals critical regulatory elements in the cardiac myosin light chain 2
948 promoter of zebrafish. Dev Dyn. 2003;228: 30–40. doi:10.1002/dvdy.10356

949 91. Aanstad P, Santos N, Corbit KC, Scherz PJ, Trinh LA, Salvenmoser W, et al. The extracellular

950 domain of Smoothened regulates ciliary localization and is required for high-level Hh signaling.
951 Curr Biol. 2009;19: 1034–1039. doi:10.1016/j.cub.2009.04.053

952 92. Thompson JD, Gibson TJ, Higgins DG. Multiple sequence alignment using ClustalW and
953 ClustalX. Curr Protoc Bioinformatics. 2002;Chapter 2: Unit 2.3.
954 doi:10.1002/0471250953.bi0203s00

955 93. Kwan KM, Fujimoto E, Grabher C, Mangum BD, Hardy ME, Campbell DS, et al. The Tol2kit: A
956 multisite gateway-based construction kit forTol2 transposon transgenesis constructs. Dev Dyn.
957 2007;236: 3088–3099. doi:10.1002/dvdy.21343

958 94. Villefranc JA, Amigo J, Lawson ND. Gateway compatible vectors for analysis of gene function in
959 the zebrafish. Dev Dyn. 2007;236: 3077–3087. doi:10.1002/dvdy.21354

960 95. Lewis JL, Bonner J, Modrell M, Ragland JW, Moon RT, Dorsky RI, et al. Reiterated Wnt signaling
961 during zebrafish neural crest development. Development. 2004;131: 1299–1308.
962 doi:10.1242/dev.01007

963 96. Schindelin J, Arganda-Carreras I, Frise E, Kaynig V, Longair M, Pietzsch T, et al. Fiji: an open-
964 source platform for biological-image analysis. Nat Methods. 2012;9: 676–682.
965 doi:10.1038/nmeth.2019

966 97. D'Aniello E, Rydeen AB, Anderson JL, Mandal A, Waxman JS. Depletion of retinoic acid
967 receptors initiates a novel positive feedback mechanism that promotes teratogenic increases in
968 retinoic acid. PLoS Genet. 2013;9: e1003689. doi:10.1371/journal.pgen.1003689

969 98. Livak KJ, Schmittgen TD. Analysis of relative gene expression data using real-time quantitative
970 PCR and the 2(-Delta Delta C(T)) Method. Methods. 2001;25: 402–408.
971 doi:10.1006/meth.2001.1262

972

Supporting Information_Coppola et al.

S1 Fig.

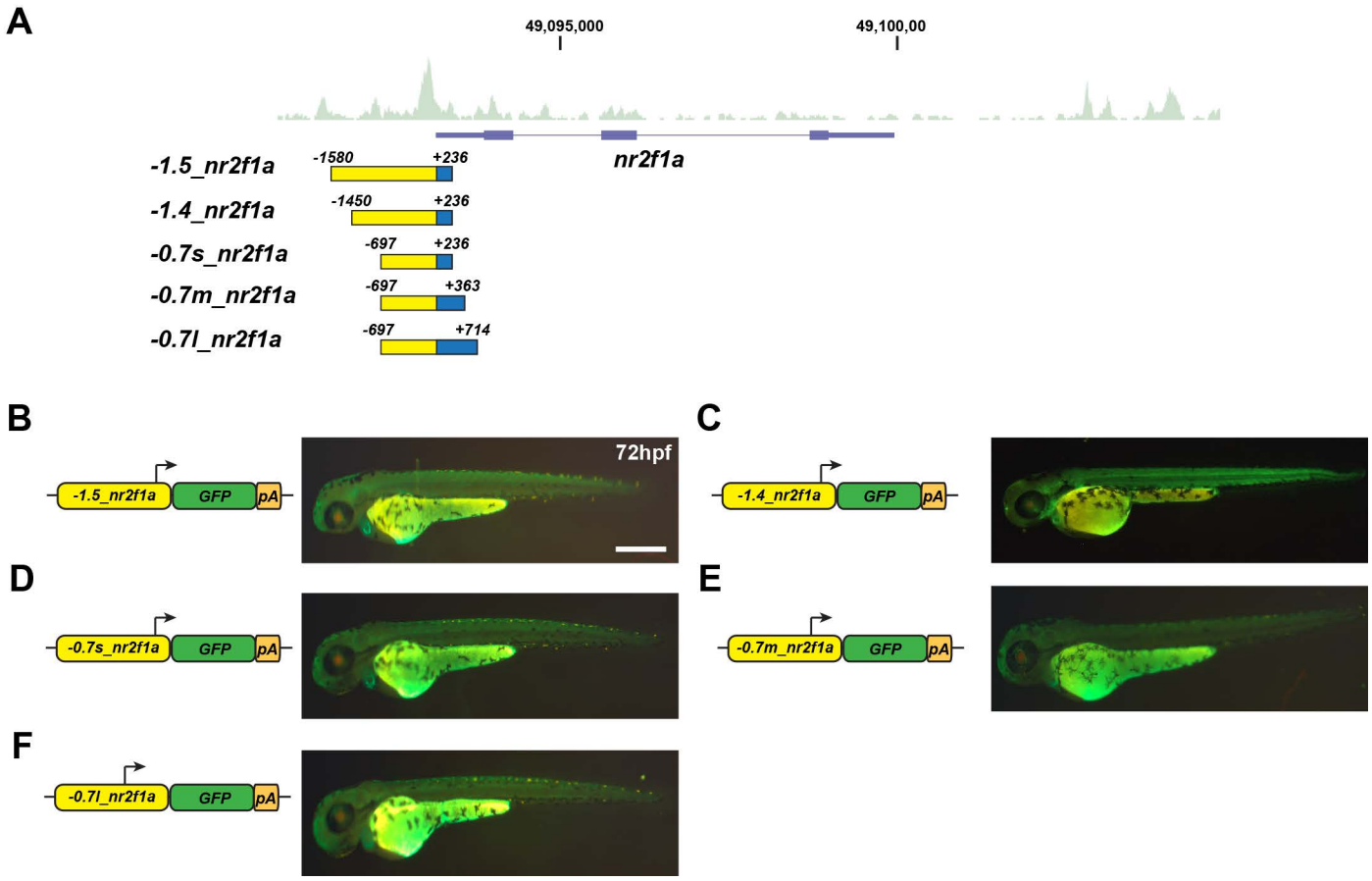

S1 Fig. The proximal promoter region of *nr2f1a* promotes broad expression in zebrafish embryos. A) Schematic of open chromatin in ACs from ATAC-seq showing the putative promoter fragments relative to the *nr2f1a* locus that were analyzed with stable transgenic lines. **B-F**) Schematics of the *nr2f1a* promoter transgenic constructs and images of representative stable transgenic lines. All the promoter constructs showed broad expression throughout the embryos. Lateral view with anterior left and dorsal upward. Scale bar: 500 μm.

S2 Fig.

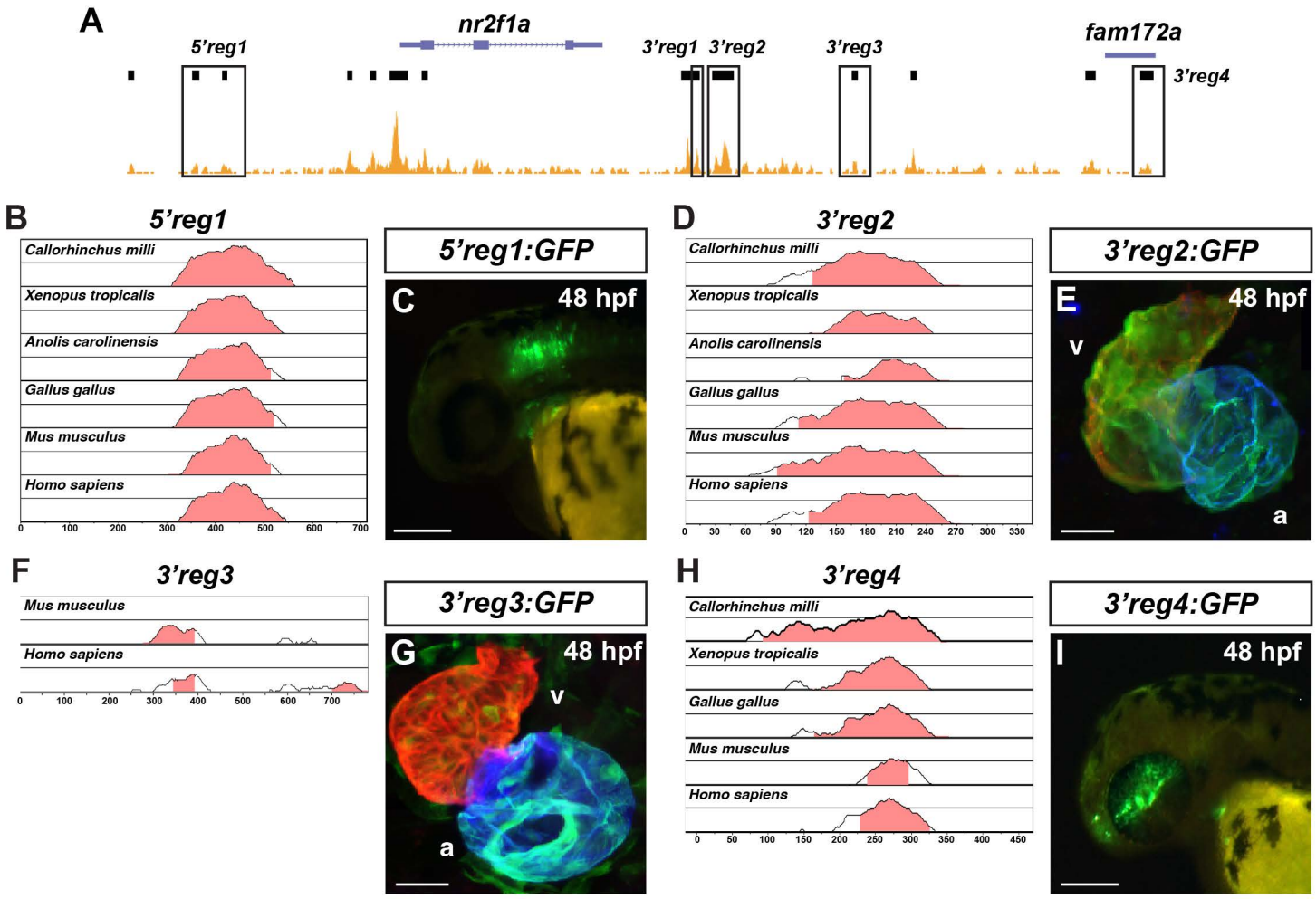

S2 Fig. *Nr2f1a* enhancers promote expression in neural tissue and the heart. A) Schematic of ATAC-seq data in ACs showing the localization of additional putative enhancers that were examined with reporters relative to the *nr2f1a* locus. **B**) VISTA plot showing conservation of the zebrafish *5'reg1-nr2f1a* enhancers with regions in *Callorhinchus milli* (Australian ghostshark), *Xenopus tropicalis* (Tropical clawed frog), *Anolis carolinensis* (Green Anole), *Gallus gallus* (chicken), *Mus musculus* (House mouse), and *Homo sapiens* (human). **C**) Image of *5'reg1:GFP* embryo with expression in the anterior hindbrain and branchial arches at 48 hpf. Lateral view is anterior to the left and dorsal upward. (n=25). Scale bar: 200 µm. **D**) VISTA plot showing conservation of the zebrafish *3'reg2-nr2f1a* enhancer with regions in *Callorhinchus milli* (Australian ghostshark), *Xenopus tropicalis* (Tropicalis clawed frog), *Anolis carolinensis* (green Anole), *Gallus gallus* (chicken), *Mus musculus* (House mouse), and *Homo sapiens* (human). **E**) Confocal image of heart at 48 hpf from *3'reg2:GFP* embryo stained for *3'reg2:GFP* (green), Vmhc (red), and Amhc (blue). V indicates ventricle. A indicates atrium. (n=21). Scale bar: 50 µm. **F**) VISTA plot showing conservation of the zebrafish *3'reg3-nr2f1a* enhancer with regions in *Mus musculus* (House mouse) and *Homo sapiens* (human). **G**) Confocal images of heart at 48 hpf from *3'reg3:GFP* embryos stained for *3'reg3:GFP* (green), Vmhc (red), and Amhc (blue). V indicates ventricle. A indicates atrium. Scale bar: 50 µm. **H**) VISTA plot showing conservation of the zebrafish *3'reg4-nr2f1a* enhancer with regions in *Callorhinchus milli* (Australian ghostshark), *Xenopus tropicalis* (Tropical clawed frog), *Gallus gallus* (chicken), *Mus musculus* (House mouse), and *Homo sapiens* (human). **I**) Image of the *3'reg4:GFP* embryo with expression in the medial eye, the anterior brain, the nasal pits, and the first branchial arch at 48 hpf (n=23). Scale bar: 200 µm. Pink in VISTA plots indicates >50% conservation of regulatory regions with the zebrafish enhancer sequence. Median lines in individual VISTA plots indicate 75% conservation. n indicates the number of embryos examined from a representative clutch. All images are of stable transgenic embryos.

S3 Fig.

A 5'reg1-nr2f1a/Nr2f1

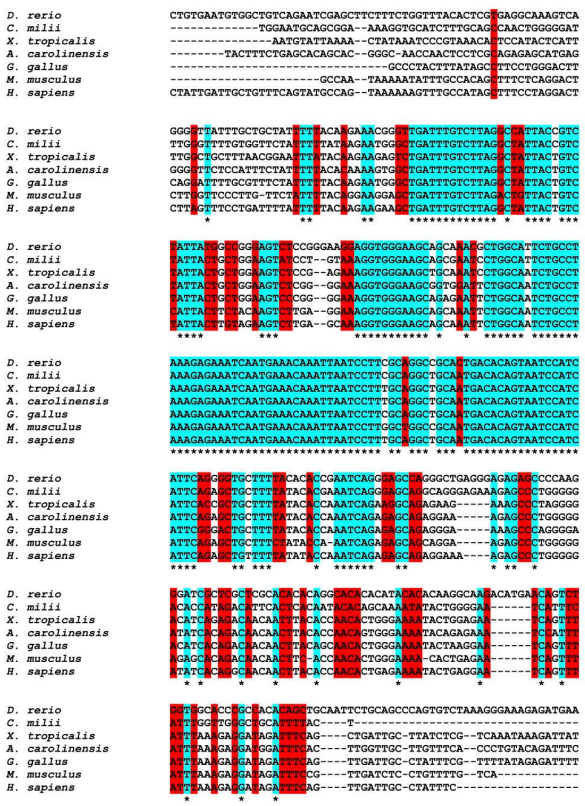

B 3'reg2-nr2f1a/Nr2f1

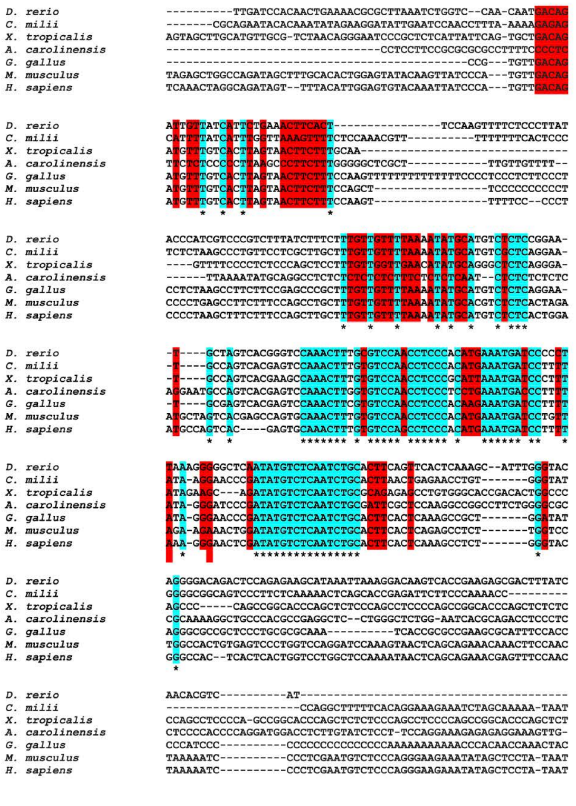

C 3'reg3-nr2f1a/Nr2f1

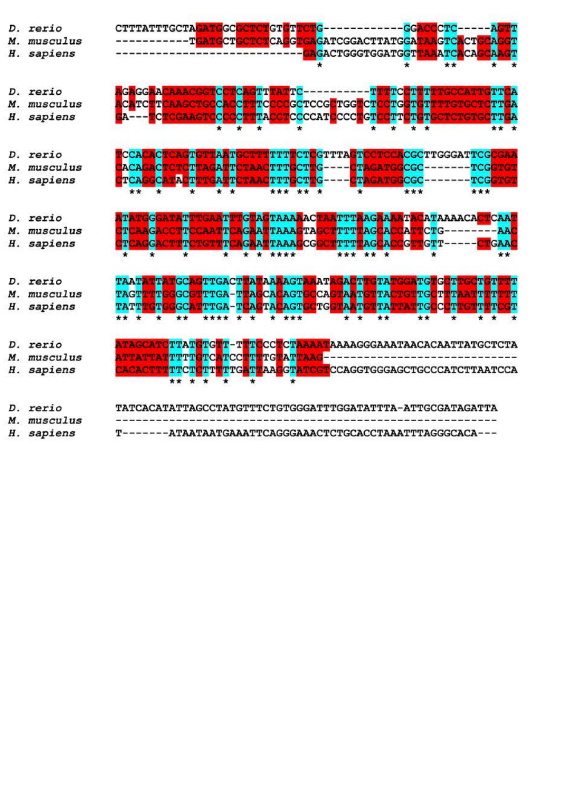

D 3'reg4-nr2f1a/Nr2f1

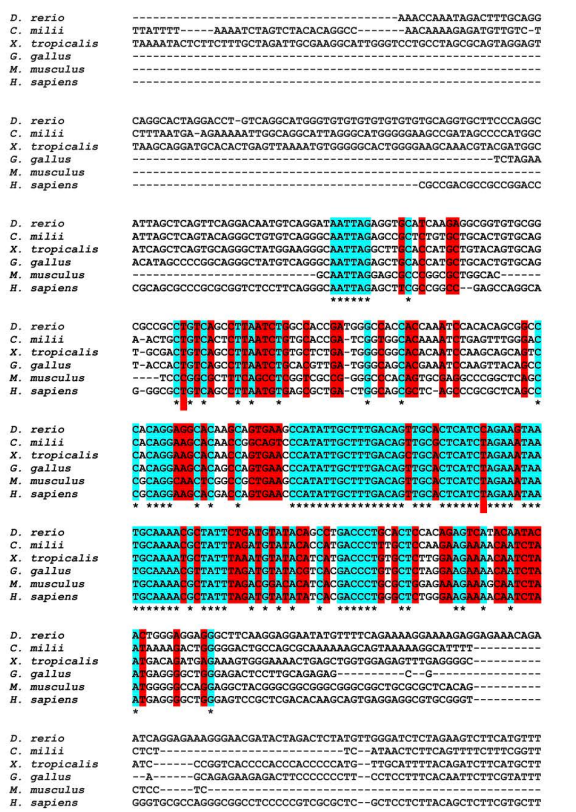

S3 Fig. Conservation of *nr2f1a* enhancer sequences in other vertebrate species. A-D) Clustal alignments of *5'reg1-nr2f1a/Nr2f1*, *3'reg2-nr2f1a/Nr2f1*, *3'reg3-nr2f1a/Nr2f1*, *3'reg4-nr2f1a/Nr2f1* between zebrafish and additional vertebrate species: *Callorhinchus milli* (Australian ghostshark), *Xenopus tropicalis* (Tropical clawed frog), *Gallus gallus* (chicken), *Anolis carolinensis* (Green Anole), *Mus musculus* (House mouse), and *Homo sapiens* (human). Turquoise indicates completely conserved nucleotides. Red indicates partially conserved nucleotides.

S4 Fig.

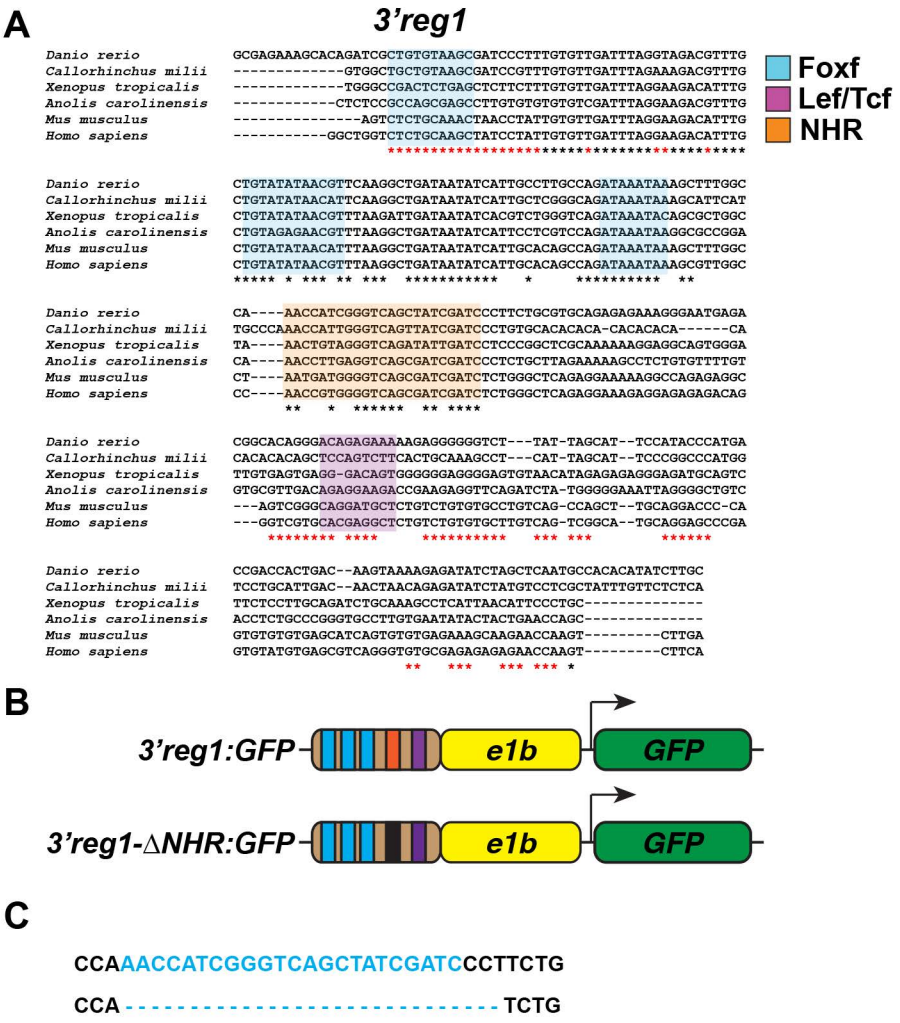

S4 Fig. The NHR site within *3'reg1* is not required to promote expression or responsive to loss of RA signaling. A) Clustal alignment of *3'reg1* with the putative NHR site highlighted, as well as Foxf1 and Lef/Tcf sites as shown in Fig. 1. **B**) Schematics of *3'reg1:GFP* reporter constructs. Foxf sites (blue), Lef/Tcf site (purple), NHR site (orange), deleted NHR site (black). **C**) Sequences showing WT NHR site and deletion of the NHR site in the *3'reg1:GFP* constructs. Deletion of the NHR site did not affect expression within the heart relative to the WT *3'reg1:GFP* construct (n=48) nor did treatment with the RA signaling inhibitor DEAB (N=33).

S5 Fig.

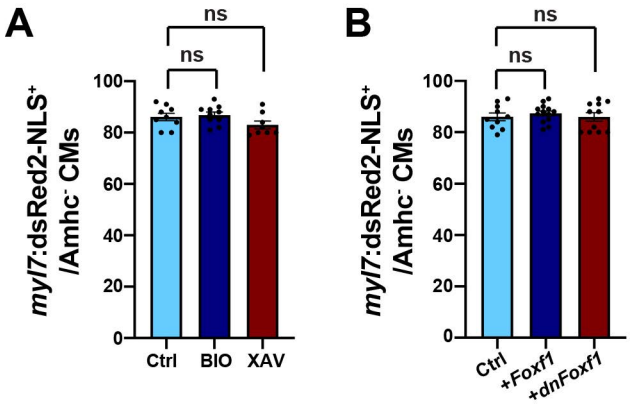

S5 Fig. Wnt and Foxf1 manipulations do not impact VC number. A) The number of VCs (*myl7*:DsRed2-NLS+/Amhc- cardiomyocytes) within the hearts of control, BIO-, and XAV-treated embryos. Control (n=9); BIO (n=10); XAV (n=8). **B**) The number of VCs (*myl7*:DsRed2-NLS+/Amhc- cardiomyocytes) within the hearts of control, *Foxf1* mRNA, and *dnFoxf1* mRNA-injected embryos. Control (n=10); *Foxf1* mRNA (n=13); *dnFoxf1* mRNA (n=11). Error bars in graphs indicate s.e.m..

S6 Fig.

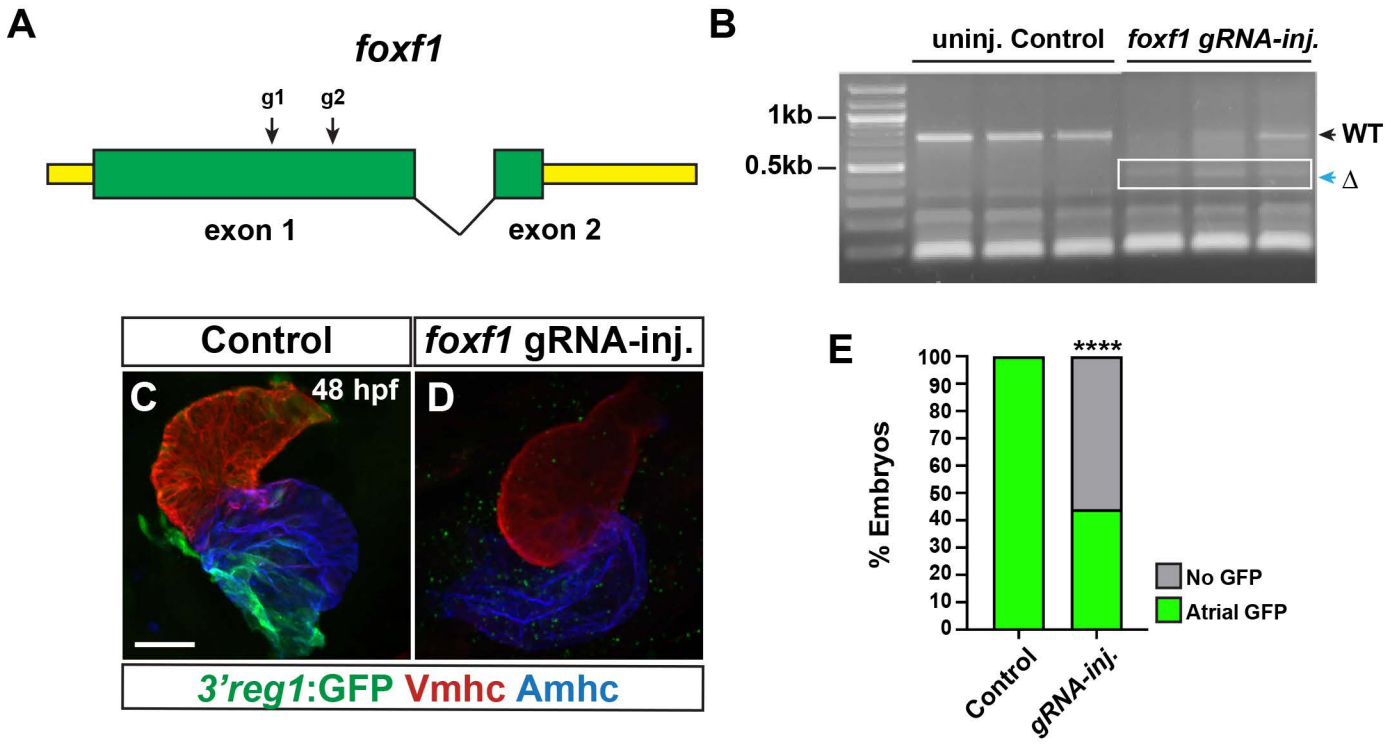

S6 Fig. Loss of *foxf1* in zebrafish leads to a reduction in *3'reg1:GFP* expression within hearts. **A**) Schematic showing the location of the guides (arrow) spaced ~200 bp apart in the first exon of zebrafish foxf1. **B**) PCR showing the efficacy of guides in creating an ~200 bp deletion and eliminating the WT band for foxf1 within representative injected *3'reg1:GFP* embryos. **C**) Confocal images of hearts from control and *foxf1* CRISPR-Cas12 injected transgenic *3'reg1:GFP* embryos stained for *3'reg1*:GFP (green), Vmhc (red), and Amhc (blue). Scale bars: 50 μm. D) The percentage of control uninjected and *foxf1* crispant *3'reg1:GFP* embryos with expression in the heart. Control (n=44); *foxf1* crispant (n=48). **** indicate $P < 0.0001$.

S7 Fig.

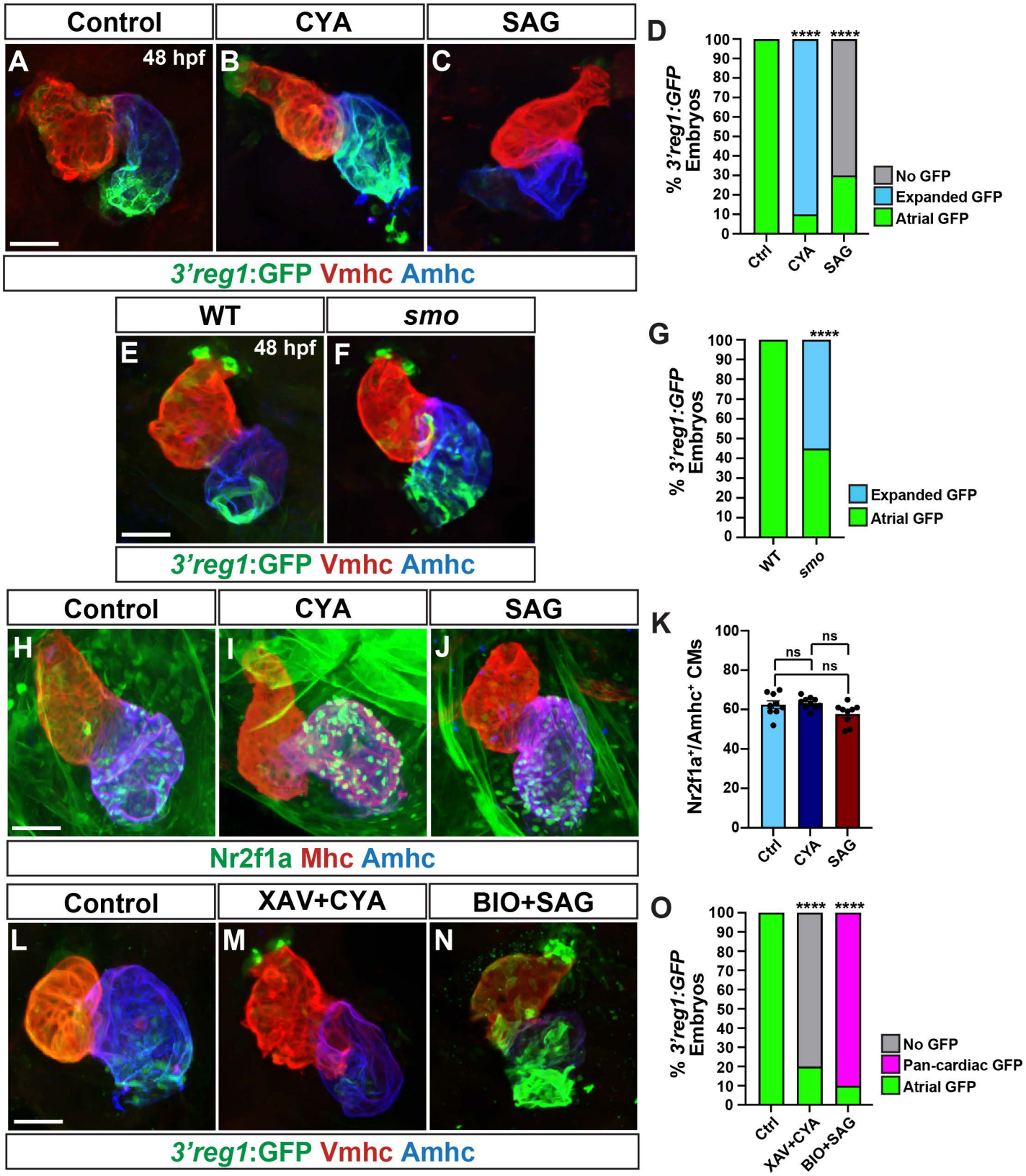
Control
CYA
SAG
A
48 hpf
B
C
3'reg1:GFP Vmhc Amhc
D
% 3'reg1:GFP Embryos
****
****
No GFP
Expanded GFP
Atrial GFP
Ctrl
CYA
SAG
WT
smo
E
48 hpf
F
3'reg1:GFP Vmhc Amhc
G
% 3'reg1:GFP Embryos
****
Expanded GFP
Atrial GFP
WT
smo
Control
CYA
SAG
H
I
J
Nr2f1a Mhc Amhc
K
Nr2f1a+/Amhc+ CMs
ns
ns
ns
Ctrl
CYA
SAG
Control
XAV+CYA
BIO+SAG
L
M
N
3'reg1:GFP Vmhc Amhc
O
% 3'reg1:GFP Embryos
****
****
No GFP
Pan-cardiac GFP
Atrial GFP
Ctrl
XAV+CYA
BIO+SAG

S7 Fig. Hh signaling represses *3'reg1:GFP* expression within the hearts. A-C) Confocal images of hearts from untreated control, CYA-treated, SAG-treated, XAV+CYA-treated, and BIO+SAG-treated transgenic *3'reg1:GFP* embryos stained for *3'reg1*:GFP (green), Vmhc (red), and Amhc (blue). **D**) The percentage of *3'reg1*:GFP embryos treated with CYA and SAG that had expanded or inhibited reporter expression within the atria. Control (n=31); CYA (n=44); SAG (n=98). **E,F**) Confocal images of hearts from WT sibling and *smo* mutant *3'reg1:GFP* embryos stained for *3'reg1*:GFP (green), Vmhc (red), and Amhc (blue). **G**) The percentage of WT and *smo 3'reg1*:GFP embryos that had expanded reporter expression within their atria. Control (n=24); *smo* (n=51). **H-J**) Confocal images of hearts from untreated control, CYA-treated, and SAG-treated stained for Nr2f1a (green), Mhc (red), and Amhc (blue). Scale bars: 50 μm. **K**) The number of Nr2f1a+/Amhc+ cardiomyocytes in the hearts of untreated control, CYA-treated, and SAG-treated embryos. Control (n=8); CYA (n=10); SAG (n=9). **L-N**) Confocal images of hearts from untreated control, XAV+CYA-treated, and BIO+SAG-treated transgenic *3'reg1:GFP* embryos stained for *3'reg1*:GFP (green), Vmhc (red), and Amhc (blue). **O**) The percentage of *3'reg1*:GFP embryos treated concurrently with XAV+CYA and BIO+SAG that had expanded or inhibited reporter expression within the atria. Control (n=23); CYA+XAV (n=99); SAG+BIO (n=109). Scale bars: 50 μm. Error bars in graph indicate s.e.m.. **** indicate $P < 0.0001$. ns indicates not a statistically significant difference.

S8 Fig.

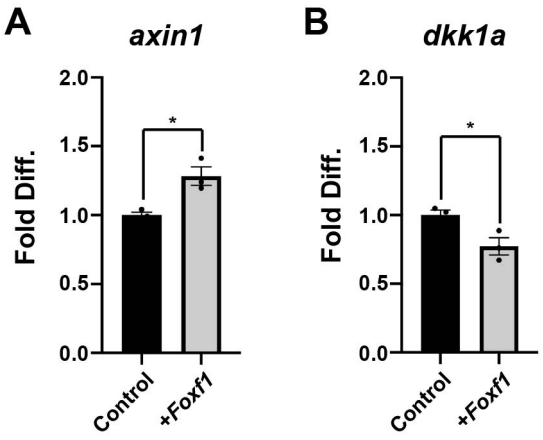

S8 Fig. Foxf1 is sufficient to promote an increase in Wnt signaling in embryos at 24 hpf. A,B) RT-qPCR for *axin1* and *dkk1a* in 24 hpf embryos injected with *Foxf1* mRNA. Fold difference is relative to *β-actin*. Error bars in graphs indicate s.e.m.. **** indicate $P < 0.05$.

S9 Fig.

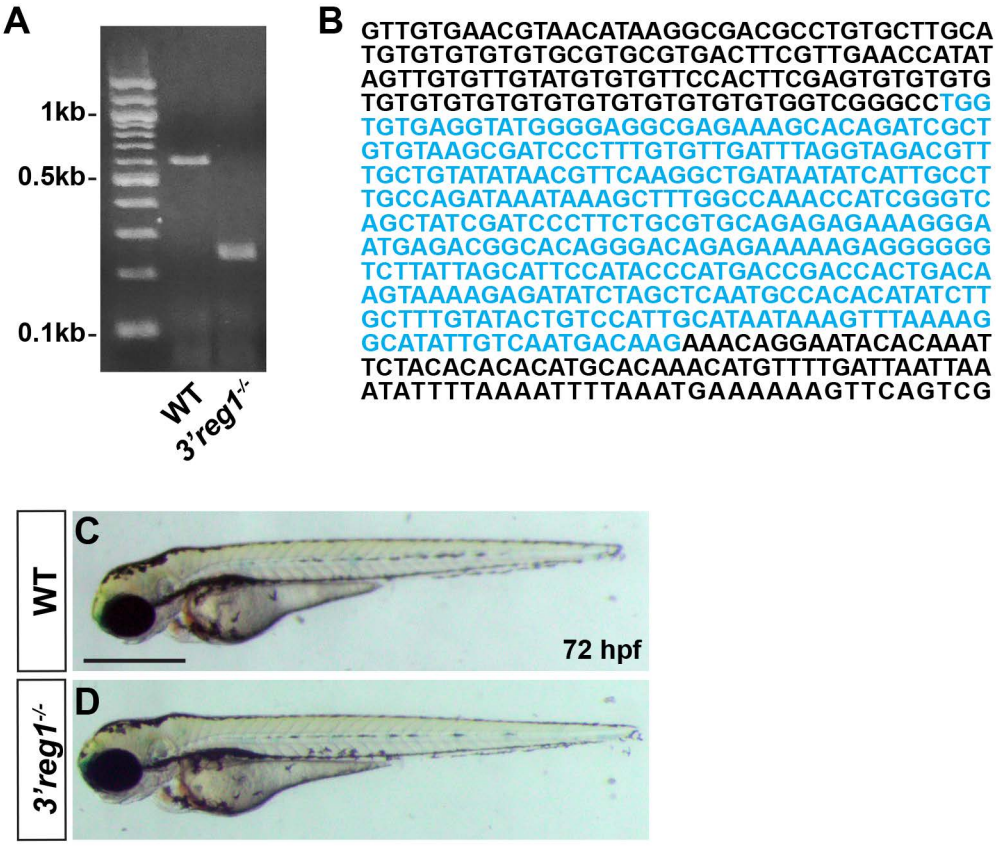

S9 Fig. Zebrafish *3'reg1*$^{-/-}$ embryos. A) PCR from WT and *3'reg1* embryos. The WT *3'reg1* PCR product is 594 bp. The PCR product for the *3'reg1* deletion is 354 bp. **B**) *3'reg1* sequence showing the deleted sequence (blue). **C,D**) Representative WT and *3'reg1*$^{-/-}$ embryos at 72 hpf. Lateral views with anterior leftward and dorsal upward. *3'reg1*$^{-/-}$ embryos do not have an overt phenotype. Scale bar: 500 μm.

S10 Fig.

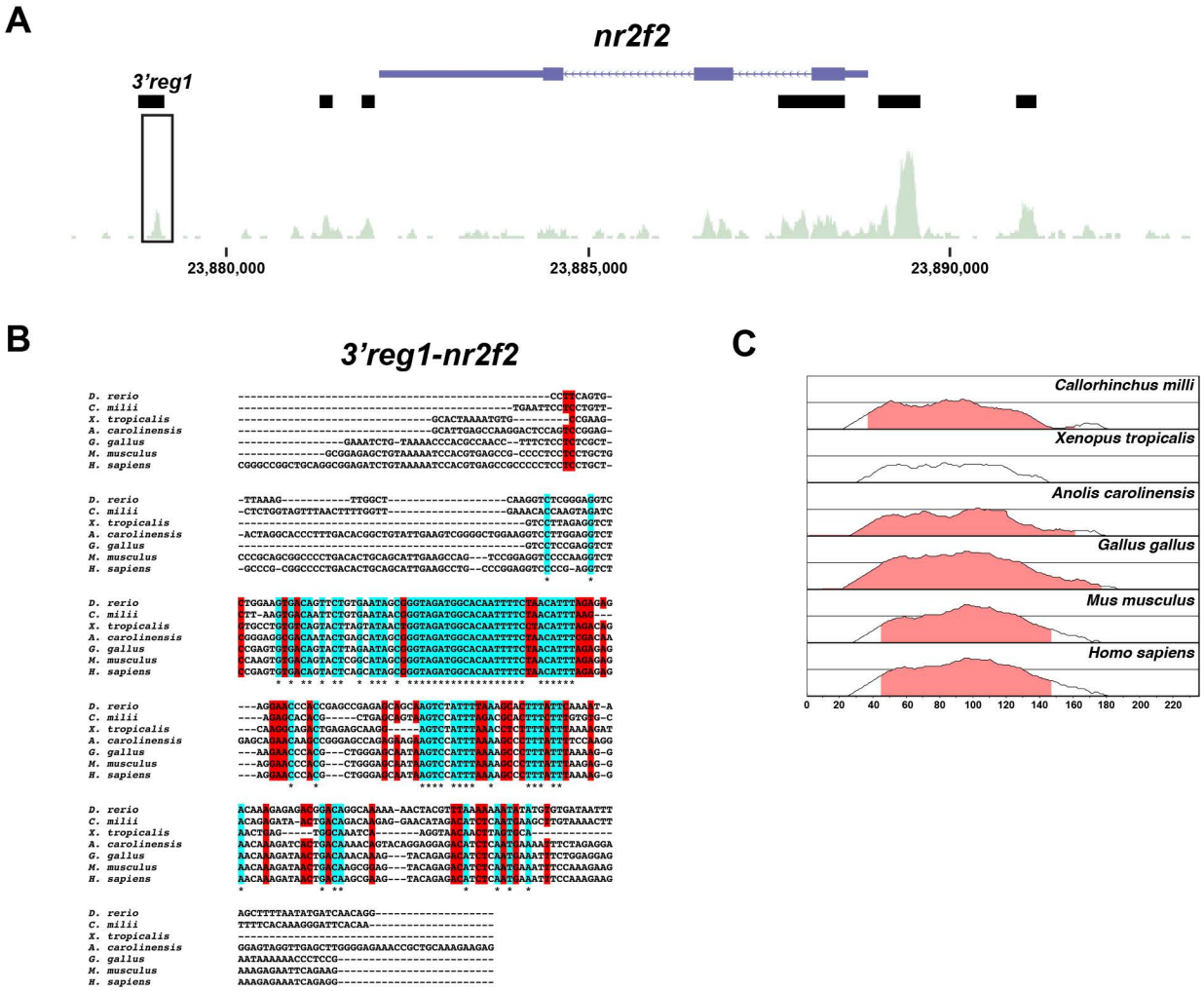

S10 Fig. *3'reg1-nr2f2* enhancer is conserved in gnathostomes. A) Schematic of ATAC-seq data in ACs showing the localization of the putative *3'reg1-nr2f2* enhancer relative to the *nr2f2* locus. **B**) Clustal alignment of *3'reg1-nr2f2* from *Danio rerio* (zebrafish), *Callorhinchus milli* (Australian ghostshark), *Xenopus tropicalis* (Tropical clawed frog), *Anolis carolinensis* (Green Anole), *Gallus gallus* (chicken), *Mus musculus* (House mouse), and *Homo sapiens* (human). Turquoise indicates completely conserved nucleotides. Red indicates partially conserved nucleotides. **C**) VISTA plot showing conservation of the zebrafish *3'reg1-nr2f2* enhancer with regions in *Callorhinchus milli* (Australian ghostshark), *Xenopus tropicalis* (Tropicalis clawed frog), *Anolis carolinensis* (green Anole), *Gallus gallus* (chicken), *Mus musculus* (House mouse), and *Homo sapiens* (human). Pink indicates >50% conservation of regulatory regions with zebrafish *3'reg1*. Median lines in individual VISTA plots indicate 75% conservation.